

intermittent benzene inhalation was found to induce oscillatory proliferation of BM cells to counter any additional epigenetic hematopoietic neoplastic impacts (Yoon *et al.*, 2001). DNA repair systems would naturally be affected by such epigenetic neoplastic impacts during intermittent oscillatory changes, and the weak oxidative stress induced by benzene metabolites has also been found to influence neoplastic transformation (Li *et al.*, 2006; Snyder, 2007).

There remain some data gaps among the experimental animal studies of benzene-induced leukemias in this area. First, the incidence of HPNs after low-level benzene exposure in wild-type mice is threshold like and equivocal, despite the significant genotoxicity of benzene even at doses lower than 1 ppm and the related decrease in the number of hematopoietic progenitor cells (Lan *et al.*, 2004). Second, there is a nonlinear-plateaued increase in the incidence of HPNs despite the lower toxicity of benzene (large LD<sub>50</sub> value of 1000–10,000 mg/kg body weight; WHO, 2003). Third, there is a lack of acute myeloid leukemias (AMLs) in most of the experimental studies in mice, despite the high frequency of AMLs observed in human cases of occupational exposure to benzene.

Accordingly, reevaluation is required in order to resolve these data gaps. The equivocal response of the induction of HPNs at low doses is hypothesized on the basis of DNA repair mechanisms in wild-type mice, while a limited increase in the incidence of HPNs at high doses is hypothesized for a highly apoptosis-sensitive subfraction in the BM. In exploring this hypothesis, *Trp53* deficiency may prove useful since this deficiency provides a cellular mechanism for the failure of DNA repair and for escape from apoptosis (French *et al.*, 2001; Hirabayashi *et al.*, 2003; MacDonald *et al.*, 2004; Storer *et al.*, 2001). *Trp53*-deficient C57BL/6 mice were used to evaluate the incidence of benzene-induced HPNs, specifically, in AMLs where there is a lack of DNA repair. Any potential increase in incidence of HPNs due to known *Trp* deficiency mechanisms may be interpreted in relation to murine AMLs. We can then compare the development of AML in these *Trp53*-deficient C57BL/6 mice to that seen in a C3H/He (AML prone) strain. This will make it feasible to identify any differences among strains regarding potentially excessive induction of leukemia associated with *Trp53* deficiency.

*Trp53*-deficient mice show increased genomic instability and deficient repair mechanism because of the absence of cell cycle arrest induced by *Trp53* after genotoxic damage. These mice, thus, provide a useful tool for examining an exaggerated neoplastic transformation after DNA damage induced by genotoxic chemicals. A marked increase in the incidence of chemical-induced cancers is potentially attributable to a genotoxic mechanism (Harvey *et al.*, 1993; Hirabayashi *et al.*, 2003; MacDonald *et al.*, 2004; Kemp *et al.*, 1994; Yoshida *et al.*, 2007). This method has also been recommended as a sensitive experimental tool for carcinogenicity bioassay of directly genotoxic carcinogens, for ionizing radiation as well as for chemicals (French *et al.*, 2001; Hirabayashi *et al.*, 2003;

MacDonald *et al.*, 2004; Storer *et al.*, 2001). However, homozygous *Trp53*-deficient mice are difficult to utilize because of the high frequency of spontaneous thymic lymphomagenesis (Hirabayashi *et al.*, 2003; MacDonald *et al.*, 2004) due to the lack of physiological apoptosis in the double-negative immature T-cell subpopulation during the developmental stage (Haines *et al.*, 2006).

Because the C3H/He strain exhibits a relatively high incidence of AML (Seki *et al.*, 1991; Yoshida *et al.*, 1996), the use of *Trp53*-deficient mice from both the C57BL/6 strain and the C3H/He strain may elucidate potential relationships and differences between benzene exposure and the development of AMLs in these two strains.

Owing to the high neoplastic sensitivity and myeloid leukemogenicity of the heterozygous *Trp53*-deficient C3H/He mice use in this study, exposure to benzene induced strain-dependent HPNs, including AMLs, in a nearly benzene dose-dependent manner, suggesting that our findings on the heterozygous *Trp53*-deficient mouse may provide a useful experimental model for studying benzene-induced hematotoxicity.

## MATERIALS AND METHODS

**Benzene.** Benzene (CAS. no. 71-43-2, MW 78.11), widely utilized as a solvent for a various organic chemicals and present in gasoline and tobacco cigarettes, was obtained from Wako Fine Chemicals (Tokyo, Japan).

**Animals.** The targeting vector for *Trp53*, a recombinant with a 2.8-kb vector containing a neomycin-resistant gene immediately before the transcriptional start site, was inserted into TT2 embryonic stem cells (heterozygous for C57BL/6 and CBA; Yagi *et al.*, 1993) to established homologous recombinant clones (Tsukada *et al.*, 1993). By generating aggregation chimeras with this recombinant clones, chimeric mice and then *Trp53*-knockout mice were established in 1987 after confirmation of the germinal transmission in *Trp53*-deficient (C57BL/6 × CBA) F1 mice (Tsukada *et al.*, 1993). General information on these recombinant mice is also found elsewhere (*Trp53*<sup>tm1Sia</sup> MGI: 1926340, Mouse Genome Informatics, 2009). The original *Trp53*-deficient (C57BL/6 × CBA) F1 mice backcrossed with C57BL/6 were transferred to the animal facility of the National Institute of Health Sciences (NIHS), Japan, in the second generation. Since then, the backcrossing with C57BL/6CrSlc was carried out for over 20 generations in 1997, followed by backcrossing with C3H/HeMsNrs in 2002. Both *Trp53*-deficient strains, C57BL/6 and C3H/He, were maintained by repeated backcrossing for each strain continuously.

This study used wild type, and homozygous and heterozygous *Trp53*-deficient male C57BL/6 and C3H/He mice were used. The heterozygous and homozygous *Trp53*-deficient mice and wild-type mice were generated by mating between heterozygous *Trp53*-deficient mice at the animal facility of NIHS, Japan. Neonates were genotyped using the primer for the targeted DNA sequence, including a partial *neo* gene at the 5' end partial exon 4, by PCR analysis using tissues obtained from the tail (Hirabayashi *et al.*, 2002; Tsukada *et al.*, 1993; Yoshida *et al.*, 2002).

Cohort studies using 8-week-old mice were conducted using 10 mice for each genotype each time. Only male mice were studied in each strain owing to the similar incidences of HPN induction in both genders and to a limited number of rooms in the animal facility with gas chromatographs for the accurate monitoring of benzene exposure concentration. C57BL/6 mice (all genotypes) totaled 76 wild-type mice, 102 heterozygous *Trp53*-deficient mice, and 86 homozygous *Trp53*-deficient mice. All the animals were randomly selected on the basis of body weight and grouped by benzene dosage (300, 100,

**TABLE 1**  
Incidences of Hematopoietic and Nonhematopoietic Diseases (histopathological types, C57BL/6 mice)

Genotype	Wild type				Heterozygous <i>Trp53</i> deficiency				Homozygous <i>Trp53</i> deficiency			
	0	33	100	300	0	33	100	300	0	33	100	300
Benzene dose	0	33	100	300	0	33	100	300	0	33	100	300
No. of mice/group	20	19	19	18	24	27	25	26	21	19	23	23
HPNs (%)	2 (10.0)	4 (21.0)	3 (15.8)	10 (55.6)*	937.5%	11(40.7)	9 (36.0)	23 (88.5)*	19 (90.5)	18 (94.7)	22 (95.7)	17 (73.9)
Thymic lymphoma (%)	0 (0.0)	0 (0.0)	2 (10.5)	5 (27.8)*	0 (0.0)	1 (3.7)	4 (16.0)	19 (73.1)*	11 (52.4)	11 (57.9)	13 (56.5)	12 (52.2)
Nonthymic lymphoma (%)	2 (10.0)	4 (21.0)	1 (5.2)	5 (27.8)	9 (37.5) <sup>a</sup>	10 (37.0)	5 (20.0)	2 (7.7)*	8 (38.1)	7 (36.8)	8 (34.8)	5 (21.7)
Myeloid leukemia (%)	0 (0.0)	0 (0.0)	0 (0.0)	0 (0.0)	0 (0.0)	0 (0.0)	0 (0.0)	2 (7.7)	0 (0.0)	0 (0.0)	1 (4.3)	0 (0.0)
Other hematopoietic disorders (%)	2 (10.0)	1 (5.2)	1 (5.2)	0 (0.0)	5 (20.8)	4 (14.8)	1 (4.0)	1 (3.8)	2 (9.5)	0 (0.0)	0 (0.0)	0 (0.0)
Malignant fibrous histiocytoma (%)	0 (0.0)	1 (5.2)	1 (5.2)	0 (0.0)	5 (20.8)	3 (11.1)	0* (0.0)	0 (0.0)*	2 (9.5)	0 (0.0)	0 (0.0)	0 (0.0)
Myeloproliferative disorders/ myelodysplastic syndrome (%)	2 (10.0)	4 (21.1) <sup>b</sup>	0 (0.0)	0 (0.0)	0 (0.0)	0 (0.0)	0 (0.0)	0 (0.0)	0 (0.0)	0 (0.0)	0 (0.0)	0 (0.0)
Aplastic anemia/marrow failure (%)	0 (0.0)	0 (0.0)	0 (0.0)	0 (0.0)	0 (0.0)	1 (3.7)	1 (4.0)	1 (3.8)	0 (0.0)	0 (0.0)	0 (0.0)	0 (0.0)
Nonhematopoietic solid tumors (%)	3 (15.0)	3 (15.8) <sup>b</sup>	8 (42.1)	2 (11.1)	6 (25.0) <sup>c</sup>	12 (44.4)	8 (32.0)	2 (7.7)	0 (0.0)	1 (5.3)	1 (4.3)	6 (26.1)*
Non-neoplastic fatal diseases (%)	13 (65.0)	11 (57.9) <sup>b</sup>	7 (36.8)	6 (33.3)	5 (20.8)	0 (0.0)	7 (28.0)	0 (0.0)*	0 (0.0)	0 (0.0)	0 (0.0)	0 (0.0)

<sup>a</sup>Mouse that has two diseases.

<sup>b</sup>Other hematopoietic disorders and nonhematopoietic solid tumors or non-neoplastic fatal diseases overlapped.

\**p* Values < 0.05 between each sham control and treated group by Fisher's exact test.

33, and 0 ppm [sham exposure control]). Table 1 shows final numbers for all mice after the start of benzene exposure.

Totals for C3H/He mice were 70 wild-type mice, 72 heterozygous *Trp53*-deficient mice, and 60 homozygous *Trp53*-deficient mice. After random selection based on body weight, the mice were divided into three groups by benzene dosage (300, 100, and 0 ppm [as sham exposure control]). Table 2 shows final numbers for all mice after the start of benzene exposure.

During the study, the mice were housed individually within stainless wire cages, placed in inhalation chambers, and were kept on a 12-h light-dark cycle. An autoclave-sterilized basal pellet diet (CRF-1, Oriental Yeast Co., Ltd, Tokyo, Japan) was provided *ad libitum*, except during the 6-h daily inhalation time, when food was withdrawn irrespective of benzene treatment. Ultraviolet-sterilized water was supplied automatically via a tube throughout the study.

All the animals were maintained in a board-approved laboratory animal facility at NIHS, Japan. All experimental protocols involving the laboratory

mice used in this study were reviewed by the Interdisciplinary Monitoring Committee for Proper Animal Use and Welfare of Experimental Animals, a peer review panel established at NIHS, and approved by the Committee for Animal Care and Use (CACU) of the NIHS with the experimental code #473-2006. All animal studies were conducted using humane protocols approved by the CACU of the NIHS, Japan.

**Benzene exposure.** The mice were divided into the sham exposure control and benzene-exposed groups and housed in 1.3-m<sup>3</sup> horizontal lamina flow inhalation chambers with a flow rate of 650 l/min and 26 ventilation times/h (Sibata Scientific Technology Ltd., Tokyo, Japan) (Li *et al.*, 2006; Yoon *et al.*, 2001, 2002, 2003). The experimental groups were exposed to benzene at 300, 100, and 33 ppm for C57BL/6 mice and at 300 and 100 ppm for C3H/He mice, 6 h/day, 5 days/week for 26 weeks. The sham exposure control mice were maintained under the same conditions without benzene inhalation. After 26

**TABLE 2**  
Incidences of Hematopoietic and Nonhematopoietic Diseases (histopathological types, C3H/He mice)

Genotype	Wild type			Heterozygous <i>Trp53</i> deficiency			Homozygous <i>Trp53</i> deficiency		
	0	100	300	0	100	300	0	100	300
Benzene dose	0	100	300	0	100	300	0	100	300
No. of mice/group	23	24	23	24	24	24	18	20	22
HPNs (%)	2 (8.7)	6 (25.0)	7 (30.4)	6 (25.0)	20 (83.3)*	25 (104.2)*	15 (83.3)	14 (70.0)	20 (90.9)
Thymic lymphoma (%)	0 (0.0)	4 (16.7)	0 (0.0)	1 (4.2)	12 (50.0)*	6 (25.0)* <sup>a</sup>	12 (66.7)	12 (60.0) <sup>a</sup>	15 (68.2) <sup>a</sup>
Nonthymic lymphoma (%)	2 (8.7) <sup>a</sup>	2 (8.3)	5 (21.7) <sup>a</sup>	3 (12.5)	6 (25.0)	10 (41.7)* <sup>a</sup>	2 (11.1)	1 (5.0)	4 (18.2)
Myeloid leukemia (%)	0 (0.0)	0 (0.0)	2 (8.7)	2 (8.3)	2 (8.3)	9 (37.5)*	1 (5.6)	1 (5.0)	1 (4.6) <sup>a</sup>
Other hematopoietic disorders (%)	1 (4.4)	6 (25.0)	2 (8.7)	0 (0.0)	1 (4.2)	0 (0.0)	0 (0.0)	4 (20.0)	2 (9.1)
Malignant fibrous histiocytoma (%)	0 (0.0)	0 (0.0)	0 (0.0)	0 (0.0)	1 (4.2)	0 (0.0)	0 (0.0)	1 (5.0)	2 (9.1)
Myeloproliferative disorders/ myelodysplastic syndrome (%)	1 (4.4)	0 (0.0)	0 (0.0)	0 (0.0)	0 (0.0)	0 (0.0)	0 (0.0)	0 (0.0)	0 (0.0)
Aplastic anemia/marrow failure (%)	0 (0.0)	6 (25.0)*	2 (8.7)	0 (0.0)	0 (0.0)	0 (0.0)	0 (0.0)	3 (15.0)	0 (0.0)
Nonhematopoietic solid tumors (%)	11 (47.8) <sup>a</sup>	5 (20.8) <sup>a</sup>	8 (34.8) <sup>a</sup>	11 (45.8)	2 (8.3)*	0 (0.0)*	0 (0.0)	2 (10.0) <sup>a</sup>	1 (4.6)
Non-neoplastic fatal diseases (%)	10 (43.5)	7 (29.2)	7 (30.4)	7 (29.2)	1 (4.2)*	0 (0.0)*	3 (16.7)	1 (5.0)	0 (0.0)

\**p* Values < 0.05 between each sham control and treated group by Fisher's exact test.

<sup>a</sup>Mouse that has two diseases.

weeks, all the animals were observed throughout their lifetime under the same conditions without benzene inhalation.

**Dose monitoring for benzene exposure.** The benzene atmosphere was generated by heating liquid benzene to 16°C to form a vapor (Sibata Scientific Technology Ltd). A gas chromatograph (Shimadzu Co., Kyoto, Japan) was used to measure benzene concentration in the chambers at 30-min intervals during daily exposures (Shimadzu Co.) (Li *et al.*, 2006; Yoon *et al.*, 2001, 2002, 2003). The temperature and humidity in the chambers were automatically controlled at 24°C ± 1°C and 55 ± 10%, respectively.

**PCR analysis for genotyping.** To detect *Trp53* wild-type and *Trp53*-deficient alleles, PCR analysis was performed using genomic DNA extracted from the tail of each mouse, and synthetic oligonucleotides were used as primers as described elsewhere (Tsukada *et al.*, 1993) and briefly here as follows. To detect the *Trp53* wild-type allele, the common 5' primer (5'-aattgacaagtatgatcca-3') and 3' primer (5'-actcctcaacatcctgggcagcaacagat-3') were used. To detect the *Trp53*-deficient allele, the common 5' primer and *neo* sequence primer (5'-gaactgcgtgcaatccatcttgcattg-3') were used.

**Lifetime observation.** All mice were monitored at least twice daily throughout their lifetime. Those showing fatal symptoms, including advanced leukemias, such as anemia with pale extremities and palpable splenomegaly, were euthanized at the agonal period and then examined hematopathologically and histopathologically. Mice that died were examined for their gross anatomical features, after which all visceral organs were fixed in 10% neutral buffered formalin for histopathological examination.

**Histopathological examination.** All visceral organs, including the thymus, spleen, sternum, and femoral BM, were fixed in 10% neutral buffered formalin for 24 h. The sternum and femoral BM were decalcified in 7.5% formic acid for 72 h. After conventional processing for dehydration, paraffin-embedded sections were stained with hematoxylin and eosin and then examined histopathologically under a light microscope (Frith *et al.*, 2001; Hirabayashi *et al.*, 1992).

**Loss of heterozygosity.** During the course of benzene-induced leukemogenesis, the remaining wild-type allele of *Trp53* remaining in heterozygous *Trp53*-deficient mice may be inactivated. The frequency of such loss of heterozygosity (LOH) was previously evaluated in mice with radiation-induced leukemias. LOH for the remaining *Trp53* allele was not examined in each group because high level of consistency (91.7%) had been identified in the leukemogenicity assay previously conducted for this strain at our laboratory (Yoshida *et al.*, 2007).

**Statistical analyses.** Survival curves data were stored in a computer and processed for statistical analysis to obtain mean survival time and SE by the Kaplan-Meier method and to evaluate statistical significance by the log-rank test using SPSS 14.1 (SPSS, Inc., Chicago, IL). To determine the cumulative incidences of diseases, Fisher's exact test was applied using Microsoft Office Excel 2003 (Microsoft, Redmond, WA). Differences were considered significant at  $p < 0.05$ .

## RESULTS

### Survival Curves with Graded Exposure Doses of Benzene Inhalation

**Experimental groups.** Kaplan-Meier survival curves for wild-type mice in comparison to the two strains (C57BL/6 and C3H/He) of heterozygous and homozygous *Trp53*-deficient mice are shown in Figures 1A–1C and Figures 1D–1F, respectively. Figures 1A–1C show data for C57BL/6 mice of different genotypes, classified into four groups on the basis of benzene exposure (33, 100, and 300 ppm, 6 h/day, 5

days/week, for 26 weeks, and 0 ppm as the sham exposure control). Figures 1D–1F show data from C3H/He mice of different genotypes classified into three groups on the basis of benzene exposure dose (100 and 300 ppm, 6 h/day, 5 days/week, for 26 weeks, and 0 ppm as the sham exposure control).

**C57BL/6 strain.** The mean survival time for C57BL/6, wild-type mice in the sham exposure control group, was 629 ± 40 days (mean ± SE) after the start of the experiment (Fig. 1A). The mean survival time for the wild-type mice in the 33- and 100-ppm exposure groups was 635 ± 40 and 550 ± 41 days, respectively, and the mean survival times for wild-type mice in the 300-ppm exposure group was 346 ± 30 days (mean ± SE). Survival time decreased proportionally with increasing benzene exposure except for the slight overlapping of survival curves for the 33-ppm and the sham exposure control groups.

Among heterozygous *Trp53*-deficient mice in the 300-ppm exposure group (Fig. 1B), the survival curve shows a rapid decrease in the number of surviving mice. Mean survival time in this group was 163 ± 9 days (mean ± SE) after the start of exposure, in comparison to 346 ± 30 days in the wild-type mice. Thus, the mean survival times for the heterozygous *Trp53*-deficient group and the wild-type group, both exposed to 300 ppm, were 347 and 283 days, respectively, shorter than the corresponding sham exposure control groups (510 ± 25 days for the heterozygous *Trp53*-deficient group and 629 ± 40 days for the wild-type group).

**C3H/He strain.** In the C3H/He wild-type sham exposure group, survival time was 590 ± 33 days (mean ± SE) after the start of exposure (Fig. 1D). Mean survival time in the wild-type 100-ppm exposure group was 495 ± 39 days and in the wild-type 300-ppm exposure group was 353 ± 35 days (mean ± SE in both cases). In contrast, within the heterozygous *Trp53*-deficient group exposed to 300-ppm benzene by inhalation, the first death occurred about 71 days after the start of exposure, and mean survival time ± SE was 117 ± 5 days (Fig. 1E).

**Homozygous *Trp53*-deficient mice.** All mice in both strains with homozygous *Trp53* deficiencies died relatively soon (Figs. 1C and 1F), with mean survival times ranging 16–122 days, regardless of benzene exposure including 0 ppm. All survival curves, specifically in the four C57BL/6 groups, crossed or nearly crossed each other, except for longer survival in a small number of mice (less than 5%) in the 100-ppm exposure group. We attribute this to primarily thymic lymphomas that originate in double-negative CD4/CD8 cells lacking apoptosis, so our findings in homozygous *Trp53*-deficient mice have been omitted from further discussion. In the C3H/He mice, however, Kaplan-Meier comparison showed a statistically significant difference in survival curves between the 300-ppm exposure group and the sham exposure as determined by the log-rank test ( $p = 0.002$ , data not shown).

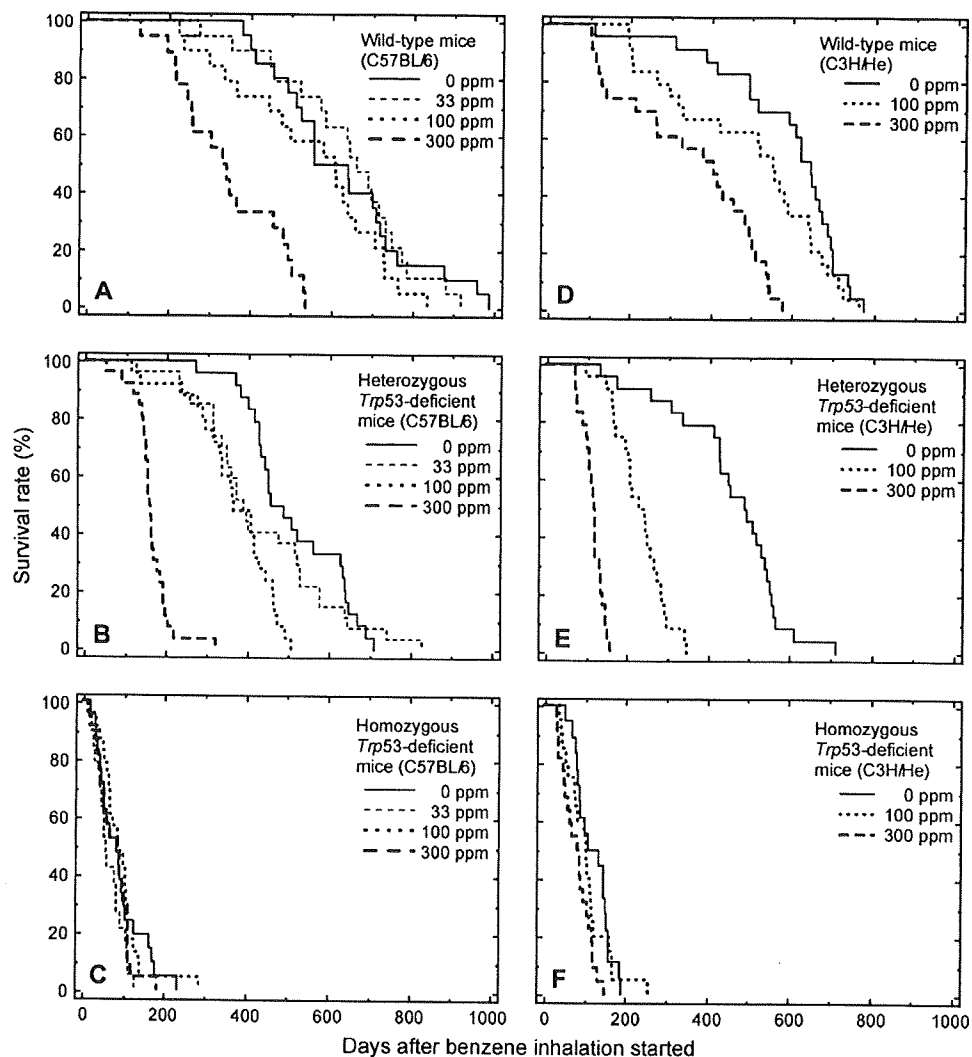


**FIG. 1.** Survival rates (%) are plotted on the vertical axis and survival time (days) after benzene inhalation on the horizontal axis, using (A)–(C) for C57BL/6 mice and (D)–(F) for C3H/He mice, with (A) and (D) for wild-type mice, (B) and (E) for heterozygous *Trp53*-deficient mice, and (C) and (F) for homozygous *Trp53*-deficient mice. Bold dotted lines for 300-ppm exposure group, regular dotted line for 100-ppm exposure group, fine dotted lines for 33-ppm exposure group, and solid line for sham exposure control. Statistical significance by log-rank test: (A) 0 versus 300 ppm,  $p = 4.7 \times 10^{-06}$ , 33 versus 300 ppm,  $p = 8.3 \times 10^{-06}$ , 100 versus 300 ppm,  $p = 4.9 \times 10^{-04}$ ; (B) 0 versus 300 ppm,  $p = 1.4 \times 10^{-10}$ ; 33 versus 300 ppm,  $p = 4.8 \times 10^{-10}$ ; 100 versus 300 ppm,  $p = 2.2 \times 10^{-08}$ ; 0 versus 100,  $p = 1.9 \times 10^{-04}$ ; 33 versus 100 ppm,  $p = 3.5 \times 10^{-02}$ ; (C) no significant difference between groups; (D) 0 versus 300 ppm,  $p = 5.6 \times 10^{-06}$ , 100 versus 300 ppm,  $p = 1.0 \times 10^{-03}$ ; (E) 0 versus 300 ppm,  $p = 5.8 \times 10^{-06}$ ; 100 versus 300 ppm,  $p = 4.0 \times 10^{-09}$ ; 0 versus 100 ppm,  $p = 1.1 \times 10^{-07}$ ; and (F) 0 versus 300 ppm,  $p = 4.4 \times 10^{-03}$ .

#### Cumulative Deaths due to HPNs

**Benzene exposure in wild-type mice.** The cumulative incidences of HPNs in each wild-type experimental group are shown in Figure 2A (C57BL/6) and Figure 2D (C3H/He). In C57BL/6 mice, the wild-type group exposed to 300 ppm showed a gradual increase in cumulative incidence of HPNs to 55.6% by day 532. In C3H/He mice, groups exposed to 100 and 300 ppm showed somewhat lower but similar increases in HPNs to 25.0% by 554 days and 30.4% by 431 days, respectively, as seen in Figure 2A (C57BL/6) and Figure 2D

(C3H/He). With the exception of the 300-ppm exposure group of wild-type C57BL/6 mice, the incidence and onset of HPNs did not exceed 21.0% during lifetime observation (21.0% for the 33-ppm group and 15.8% for the 100-ppm groups). The maximum incidences of HPNs in the wild-type sham control group were 10.0% by 492 days in C57BL/6 mice and 8.7% by 742 days in C3H/He mice.

The first question in the present study concerned threshold-like equivocal incidence of HPNs at low-dose benzene exposure. In this regard, only the C57BL/6, 300-ppm exposure

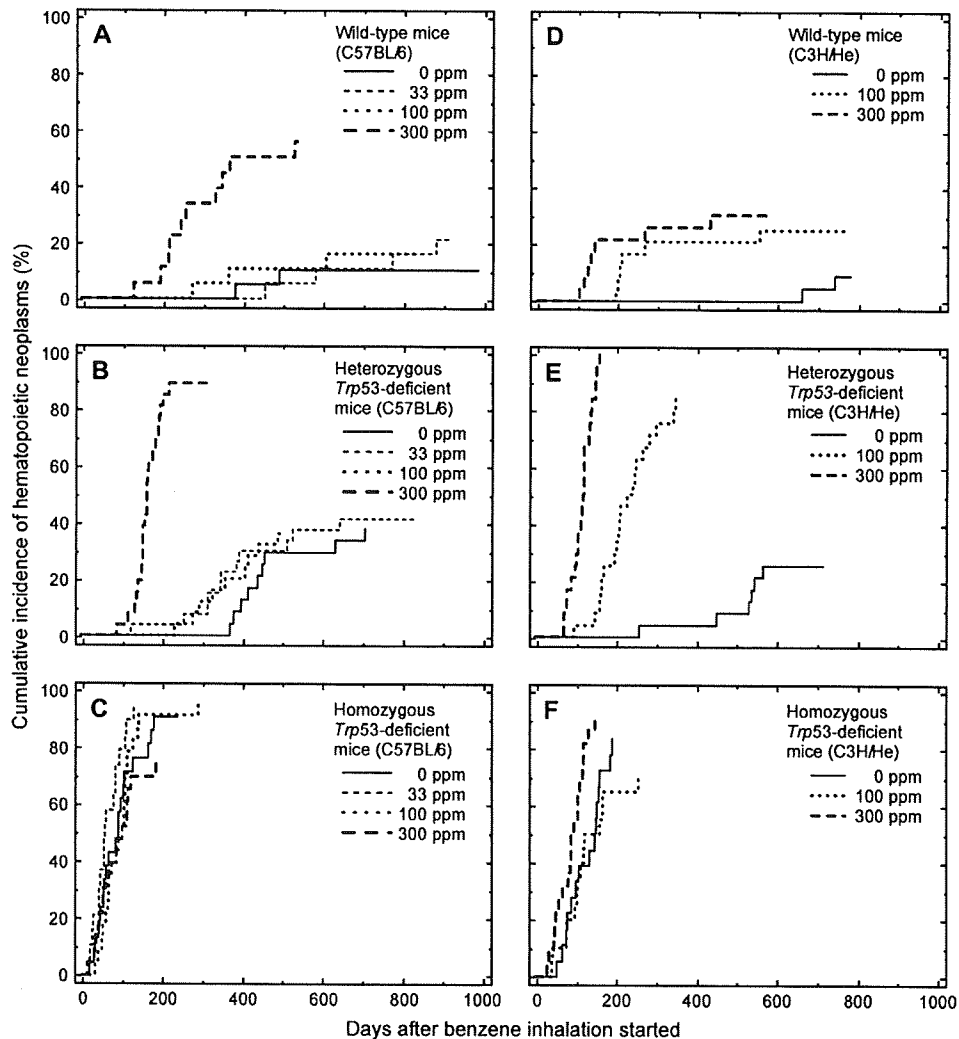


**FIG. 2.** The illustration shows the cumulative lifetime incidence of all hematopoietic malignancies (%) in C57BL/6 mice on the left (A–C) and in C3H/He mice on the right (D–F), using (A) and (D) for wild-type mice, (B) and (E) for heterozygous p53-deficient mice, and (C) and (F) for homozygous p53-deficient mice. Bold dotted line for 300-ppm exposure group, regular dotted line for 100-ppm exposure group, fine dotted line for 33-ppm exposure group, and solid line for sham exposure control. Statistical significance by log-rank test: (A) 0 versus 300 ppm,  $p = 2.7 \times 10^{-04}$ ; 33 versus 300 ppm,  $p = 4.5 \times 10^{-04}$ ; 100 versus 300 ppm,  $p = 1.8 \times 10^{-03}$ ; (B) 0 versus 300 ppm,  $p = 2.5 \times 10^{-10}$ ; 33 versus 300 ppm,  $p = 8.6 \times 10^{-10}$ ; 100 versus 300 ppm,  $p = 9.1 \times 10^{-10}$ ; (C) no significant difference between groups; (D) 0 versus 300 ppm,  $p = 7.0 \times 10^{-03}$ ; (E) 0 versus 300 ppm,  $p = 1.2 \times 10^{-11}$ ; 100 versus 300 ppm,  $p = 2.8 \times 10^{-09}$ ; 0 versus 100 ppm,  $p = 4.2 \times 10^{-08}$ ; and (F) 0 versus 300 ppm,  $p = 3.1 \times 10^{-03}$ ; 100 versus 300 ppm,  $p = 2.1 \times 10^{-02}$ .

group showed a significant differences in cumulative HPN incidence in comparison to the other C57BL/6 groups. However, findings from both the C3H/He 300-ppm and the 100-ppm exposure groups differed significantly from the sham exposure controls. These results imply that HPNs occurred at a higher than threshold level in heterozygous *Trp53*-deficient mice in both strains since such incidence was greater than and clearly separated from the incidence in each sham exposure control groups.

**Exposure in *Trp53*-deficient mice.** A high frequency of HPNs was observed in both strains of the heterozygous *Trp53*-deficient benzene exposure groups as shown in Figure 2B

(C57BL/6) and Figure 2E (C3H/He). In heterozygous *Trp53*-deficient C57BL/6 mice, a total HPN incidence of 88.5% (300 ppm) was observed from 88 to 219 days. This incidence was higher than in the sham exposure control (37.5%) and also higher than in the wild-type groups with or without benzene exposure (55.6 and 10.0%, respectively) and with earlier onset time (88 days) than in wild-type mice (130 days). The increase in incidence of HPNs between benzene exposure group and sham control was not greater in *Trp53*-deficient C57BL/6 mice than in the wild-type mice due to an increase in the late-appearing spontaneous HPNs in the *Trp53*-deficient mice, but the 50% die-off time (days) for HPNs between the former and

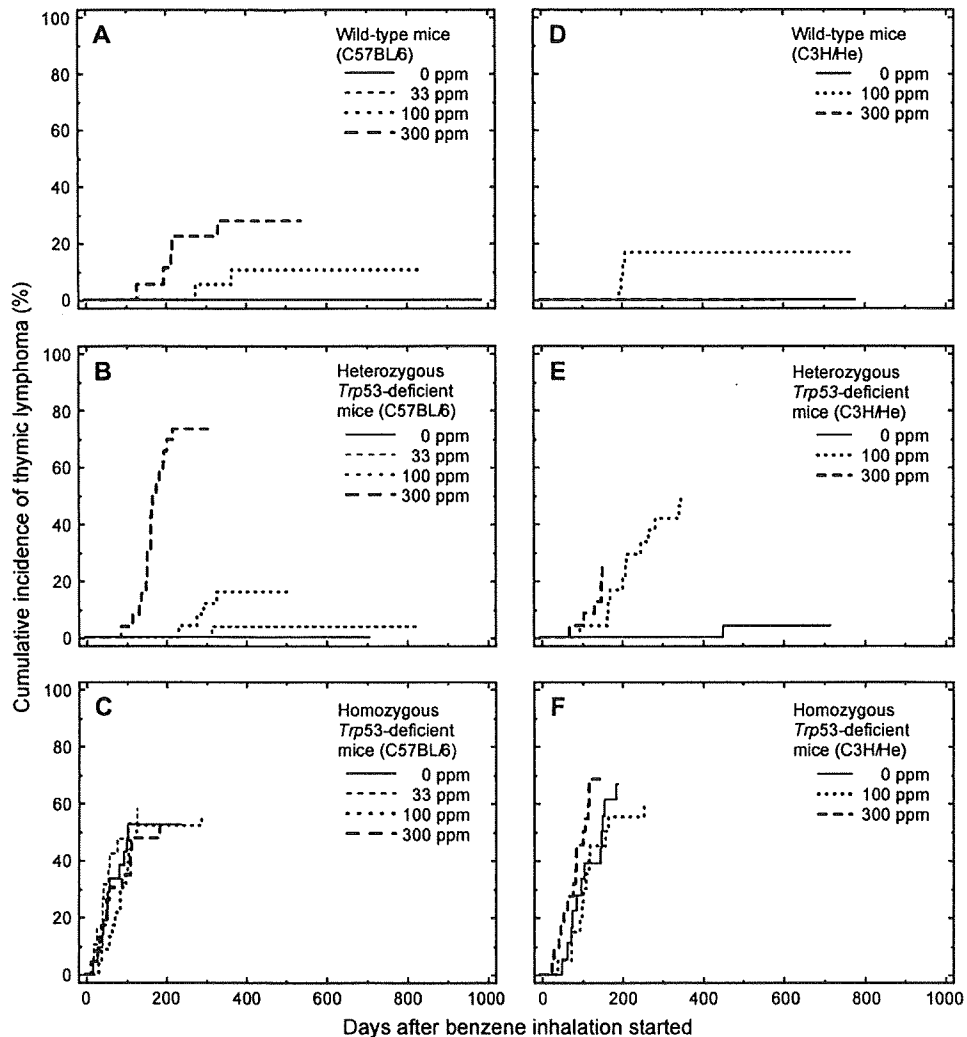


**FIG. 3.** Cumulative lifetime incidences of thymic lymphoma during the lifetime in C57BL/6 mice on the left (A–C) and C3H/He mice on the right (D–F), using (A) and (D) for the wild-type mice, (B) and (E) for heterozygous *Trp53*-deficient mice, and (C) and (F) for homozygous *Trp53*-deficient mice. Bold dotted line for 300-ppm exposure group, regular dotted line for 100-ppm exposure group, fine dotted line for 33-ppm exposure group, and solid line for sham exposure control. Statistical significance by log-rank test: (A) 0 versus 300 ppm,  $p = 9.7 \times 10^{-03}$ ; 33 versus 300 ppm,  $p = 1.2 \times 10^{-02}$ ; (B) 0 versus 300 ppm,  $p = 4.3 \times 10^{-10}$ ; 33 versus 300 ppm,  $p = 1.7 \times 10^{-10}$ ; 100 versus 300 ppm,  $p = 6.6 \times 10^{-09}$ ; 0 versus 100 ppm,  $p = 3.4 \times 10^{-02}$ ; (C) no significant difference between the two groups; (D) 0 versus 100 ppm,  $p = 4.8 \times 10^{-02}$ ; (E) 0 versus 300 ppm,  $p = 3.9 \times 10^{-05}$ ; 100 versus 300 ppm,  $p = 2.4 \times 10^{-03}$ ; 0 versus 100 ppm,  $p = 2.4 \times 10^{-06}$ ; and (F) 0 versus 300 ppm,  $p = 3.0 \times 10^{-02}$ .

the latter was significantly split in the *Trp53*-deficient mice than in the wild-type mice (266.5 vs. 184.5 days). The cumulative incidence curves for HPN in these heterozygous *Trp53*-deficient exposure groups were significantly different only in the 300-ppm exposure group, and the curves of the remaining groups occasionally overlapped for the C57BL/6 strain, but the benzene dose-dependent shortening of 50% die-out time in the 100-ppm group and the die-out time in the 100-ppm *Trp53*-deficient groups were both similarly reduced (70.5 and 70.0 days).

In heterozygous *Trp53*-deficient C3H/He mice, in contrast, the total incidence of HPNs increased in a manner dependent

on the benzene exposure dose (104.2, 83.3, and 25.0%, respectively), with earlier onset times (78, 98, and 260 days) than in wild-type mice (105, 197, and 651 days).

As illustrated in Figure 2C (C57BL/6) and Figure 2F (C3H/He), although homozygous *Trp53*-deficient mice showed slightly earlier onset of thymic lymphomas following benzene exposure, specifically in the C3H/He strain, these mice were not used for bioassay because they showed extremely early onset of highly frequent thymic lymphomas that developed spontaneously by a known mechanism, that is, development of CD4/CD8 double-negative thymic lymphomas owing to the

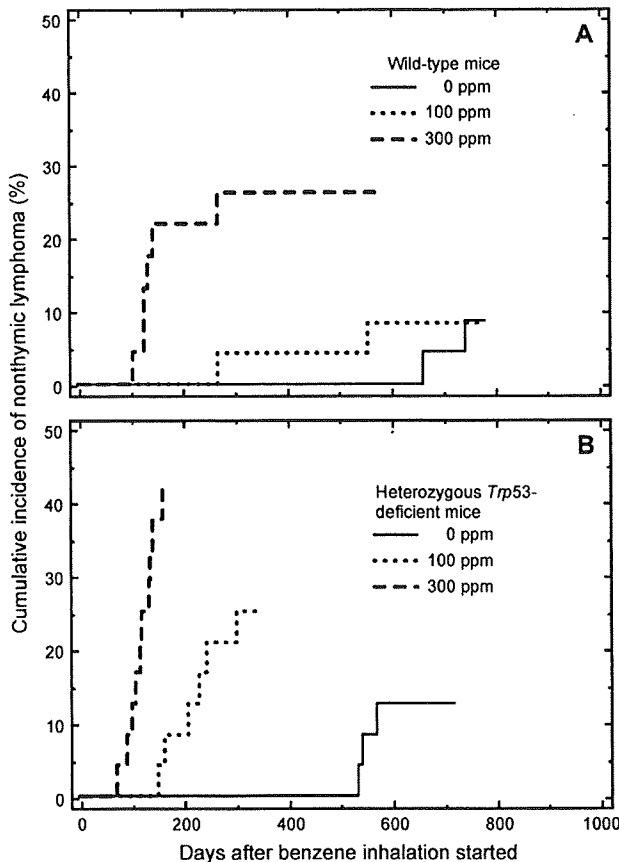


**FIG. 4.** Cumulative lifetime incidence of nonthymic (non-Hodgkin) lymphoma in C3H/He mice; wild-type mice (A) and heterozygous *Trp53*-deficient mice (B). Bold dotted line for 300 ppm, regular dotted line for 100 ppm, and solid line for sham exposure control. Statistical significance determined by log-rank test: (A) 0 versus 300 ppm,  $p = 3.1 \times 10^{-02}$ ; and (B) 0 versus 300 ppm,  $p = 1.4 \times 10^{-05}$ ; 100 versus 300 ppm,  $p = 6.4 \times 10^{-05}$ ; 0 versus 100 ppm,  $p = 4.0 \times 10^{-03}$ .

absence of physiological apoptosis in the CD4/CD8 double-negative immature T-cell population during early development (Haines *et al.*, 2006).

#### Histopathological Examination

HPNs, along with non-HPNs and non-neoplastic diseases observed in C57BL/6 mice and C3H/He mice, were classified histopathologically and tabulated separately in Table 1 for the C57BL/6 strain and Table 2 for the C3H/He strain.

**Development of thymic and nonthymic lymphoma.** As shown in these tables, in wild-type mice, only a small number of HPNs, that is, thymic lymphomas, two (10.5%) and five (27.8%) in the C57BL/6 and four (16.7%) and zero (0%) in the C3H/He, were observed in 100- and 300-ppm exposure groups, respectively (Figs. 3A and 3D). In heterozygous *Trp53*-deficient C57BL/6 mice, the number of thymic lymphomas gradually increased, that is, 0, 1 (3.7%),

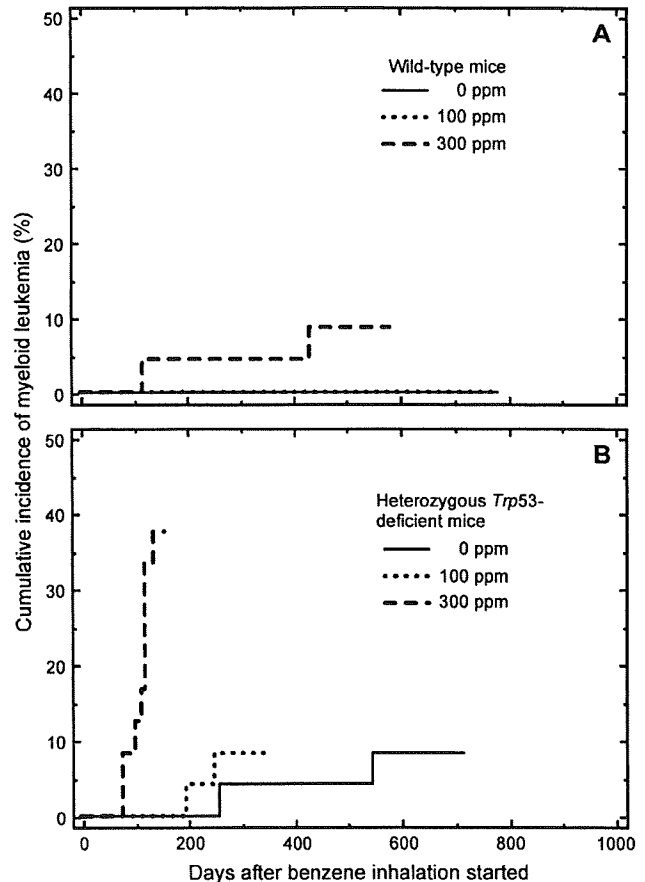


**FIG. 5.** Cumulative lifetime incidences of myelogenous leukemia during the lifetime of C3H/He mice; wild-type mice (A) and heterozygous *Trp53*-deficient mice (B). Bold dotted lines for 300 ppm, regular dotted lines for 100 ppm, and solid lines for sham exposure controls. Statistical significance determined by log-rank test: (A) no significant difference between groups; (B) 0 versus 300 ppm,  $p = 1.5 \times 10^{-04}$ ; 100 versus 300 ppm,  $p = 1.8 \times 10^{-04}$ .

4 (16.0%), and 19 (73.1%), with benzene exposure dose, that is, 0, 33, 100, and 300 ppm, respectively (Fig. 3B). Thus, the graded increase in the incidence of thymic lymphomas up to 73.1% was observed in the C57BL/6 strain, showing a linear exposure dose-response relationship. In C3H/He mice, on the other hand, the number of thymic lymphomas that developed were 1 (4.2%), 12 (50.0%), and 6 (25.0%) at benzene exposure doses of 0, 100, and 300 ppm, respectively (Fig. 3E). Thus, the number of thymic lymphomas at 300 ppm decreased and a linear exposure dose-response relationship was not observed. The mechanism underlying this observation needs to be studied.

Concerning the incidence of nonthymic (non-Hodgkin) lymphomas, a linear exposure dose-response relationship was not observed in the C57BL/6 strain, but relative increases in the incidence with the exposure dose of benzene were observed in C3H/He mice (Figs. 4A and 4B).

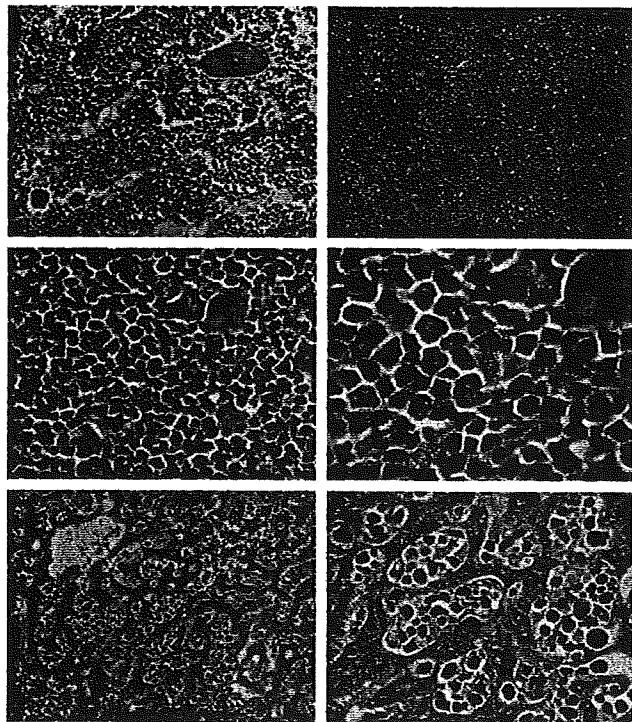


**FIG. 6.** Representative histopathological findings for AMLs developing in benzene-exposed wild-type C3H/He mice (A–F). Increased cellular density for atypical mononuclear cells with heterogeneous size distribution in sternum BM (A,  $\times 67$ ). Increased cellular density with expanding growth (arrow heads) toward surrounding splenic tissue and the lymphofollicular structures on the left (B,  $\times 34$ ). Higher magnification of neoplastic cellular component at the center of leukemic growth in (B), consisting of atypical myeloid cells with scattered bizarrely shaped myeloblastic nuclei including megakaryocytes (C,  $\times 169$ ). Higher magnification of (C), revealing detailed atypical myeloid cells, including cells with occasional doughnut-shaped nuclei (D,  $\times 312$ ). Hepatic cell cord filled with atypical mononuclear myeloblastic cell component surrounding a central vein at the upper left (E,  $\times 67$ ). Higher magnification of (E), including atypical myeloid cells, with heterogeneous size distribution, proliferating in sinusoidal spaces (F,  $\times 169$ ).

**Development of AMLs.** It is notable that heterozygous *Trp53*-deficient C3H/He mice, which are prone to AML, produced two (8.3%), two (8.3%), and nine (37.5%) AMLs in the 0-, 100-, and 300-ppm exposure groups, respectively, in comparison with wild-type mice, which produced only two (8.7%) AMLs in the 300-ppm exposure group (Fig. 5). In C57BL/6 mice, there were two AMLs in heterozygous and one in homozygous *Trp53*-deficient animals. There were essentially no significant differences in cytological and histopathological findings of AMLs between the both strains. Thus, mainly cytological and histopathological findings of AMLs developed in C3H/He mice are shown in Figure 6 (leukemias developing in wild-type mice) and Figure 7 (leukemias developing in *Trp53*-deficient mice), along with two panels (7E and 7F) from heterozygous *Trp53*-deficient C57BL/6 mice in Figure 7, bottom.

In Figure 6, atypical myeloblastic leukemic cells with irregularly bizarrely shaped nuclei, occasionally including

doughnut-shaped nuclei as shown in Figures 6C and 6D, suggest a myelogenous origin in C3H/He mice. The same atypical myeloid cells with a heterogeneous size distribution were observed to invade hepatic sinusoidal spaces (Figs. 6E and 6F). In wild-type mice, AMLs developed only in the C3H/He mice and not in the C57BL/6 mice.

Owing to the function of *Trp53* during the early developmental stage, a prominently lesser extent of differentiation was noted in AMLs developing in *Trp53*-deficient mice. Namely, as shown in Figure 7, the cytopathological and histopathological characteristics of leukemic cells in both heterozygous *Trp53*-deficient C3H/He mice (Figs. 7A–D) and C57BL/6 mice (Fig. 7E) revealed more immature blastic cells with less differentiation than leukemic cells in wild-type mice (Fig. 6). Representative atypical myeloblastic cells possessing trace peroxidase granules in the cytoplasm are shown in Figure 7B (inset, bottom). Nevertheless, some doughnut-shaped nuclei similar to those of cells with myeloid lineages were very occasionally observed in the C57BL/6 strain (Fig. 7E, inset, top and bottom).

#### *HPNs in Relationship to Benzene Exposure Dose*

The exposure dose range for benzene hematotoxicity is narrow, specifically for the induction of HPNs. Higher benzene exposure may produce a larger number of hematopoietic neoplastic candidates but simultaneously seems to decrease the number of hematopoietic progenitor cells, that is, potential targets for the induction of HPNs. Figures 8A and 8B (for C57BL/6 mice) and Figures 8C and 8D (for C3H/He mice) illustrate the relationship between the incidence of HPNs and graded increased benzene exposure.

In C57BL/6 mice, the increase in the total incidence of HPNs was only significant in both the 300-ppm exposure groups for wild-type and the heterozygous *Trp53*-deficient mice. Each histological type showed a statistically significant increase in the incidence of thymic lymphoma at 300-ppm exposure in comparison to sham exposure (Table 1). There was no statistically significant increase in HPN incidence in either the 33- or 100-ppm exposure group in comparison to spontaneous HPNs in the sham exposure groups, possibly due to the competitive increase in the incidence of non-HPNs.

In the C3H/He mice, however, the total incidence curve for HPNs in wild-type mice showed a gradual increase reaching a plateau/peak in the wild-type 100- and 300-ppm exposure groups (Fig. 8C). The heterozygous *Trp53*-deficient mice showed a significant increase (\*) in HPN incidence in the 100- and 300-ppm exposure groups, reaching up to 100% in the latter group (Fig. 8D).

## DISCUSSION

In this research, we sought answers to three questions. For the first question regarding the equivocal induction of HPNs at



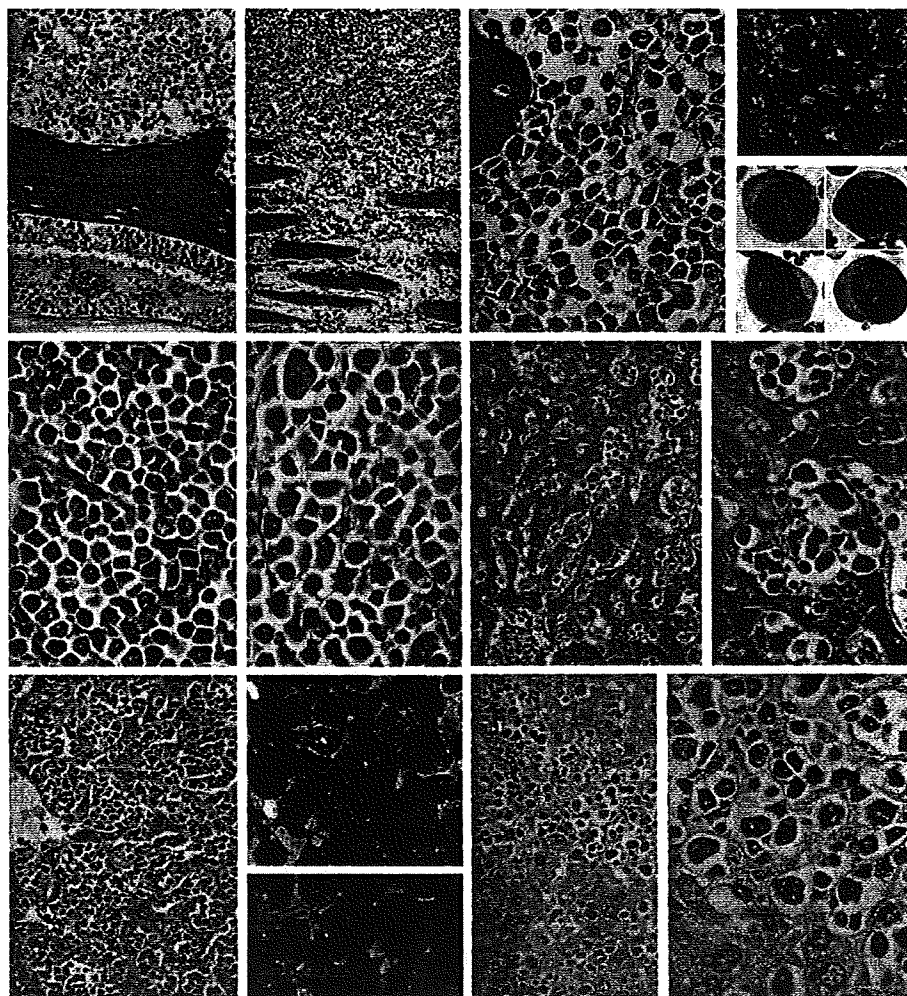


**FIG. 7.** Representative histopathological and cytopathological findings for AML developing after benzene exposure in heterozygous *Trp53*-deficient C3H/He and C57BL/6 mice: AML in femoral BM (A, left  $\times 67$ ) and its periosteal, intramuscular expansion, and infiltration into growth against surrounding soft part of femoral bone (A, right  $\times 34$ ). Higher magnification of atypical myeloid cells with widely heterogeneous size distribution and marked cellular atypia (B, left  $\times 169$ ). Imprint smear of hyperchromatic myeloblastic cells (B, inset top  $\times 253$ ) and representative characteristics of leukemic cells in smear showing atypical immature myeloblastic cells with trace evidence of intracytoplasmic peroxidase granulation (B, inset, upper row  $\times 494$  and lower row  $\times 643$ ). Atypical myeloid cellular component, proliferating in splenic white pulp for *Trp53*-deficient C3H/He mice (C, left  $\times 169$ ) and at higher magnification (C, right  $\times 253$ ). Hepatic trabecular infiltration of myeloid cells in liver of *Trp53*-deficient C3H/He mice (D, left  $\times 67$ ) and at higher magnification (D, right  $\times 169$ ). Atypical myeloid cell proliferation in liver of *Trp53*-deficient C57BL/6 mice (E, left  $\times 67$ ), atypical immature myeloid cells (E, right, top  $\times 337$ ), and tissue imprint smear from terminal stage of spleen with immature mononuclear myeloblastic cells (E, right, bottom  $\times 337$ ). Representative nonthymic malignant lymphoma, infiltrating into hepatic sinusoidal spaces (F, left  $\times 67$ ) with higher magnification of expansive growth of cerebriform bizarrely shaped cells (F, right  $\times 169$ ) in *Trp53*-deficient C57BL/6 mice.

low dose of benzene exposure, we found that heterozygous *Trp53*-deficient mice in both strains showed a higher than threshold incidence of HPNs at lower doses, as described in the "Results" section. We attribute this to the mechanism of *Trp53*-dependent repair for DNA damage induced by benzene exposure. Our second question related to the nonlinear plateau in the incidence of HPNs at high dose of benzene exposure. We found that *Trp53*-deficient mice in both strains produced a fairly high incidence of HPNs up to 100%, including 38% of AMLs in C3H/He mice exposed to benzene 300 ppm in

comparison with an incidence of only 9% in wild-type mice exposed to the same dose. These results suggest that the nonlinear plateau in the incidence of HPNs at high benzene exposure may be caused by a decrease in neoplastic target cells due to *Trp53*-dependent escape from apoptosis in wild-type mice. In addition to benzene-mediated genotoxicity, the development of HPNs generally requires an epigenetic process that does not exhaust but maintains hematopoietic stem/progenitor cells, that is, the target cells for hematopoietic neoplastic development. An excessive decrease in the number

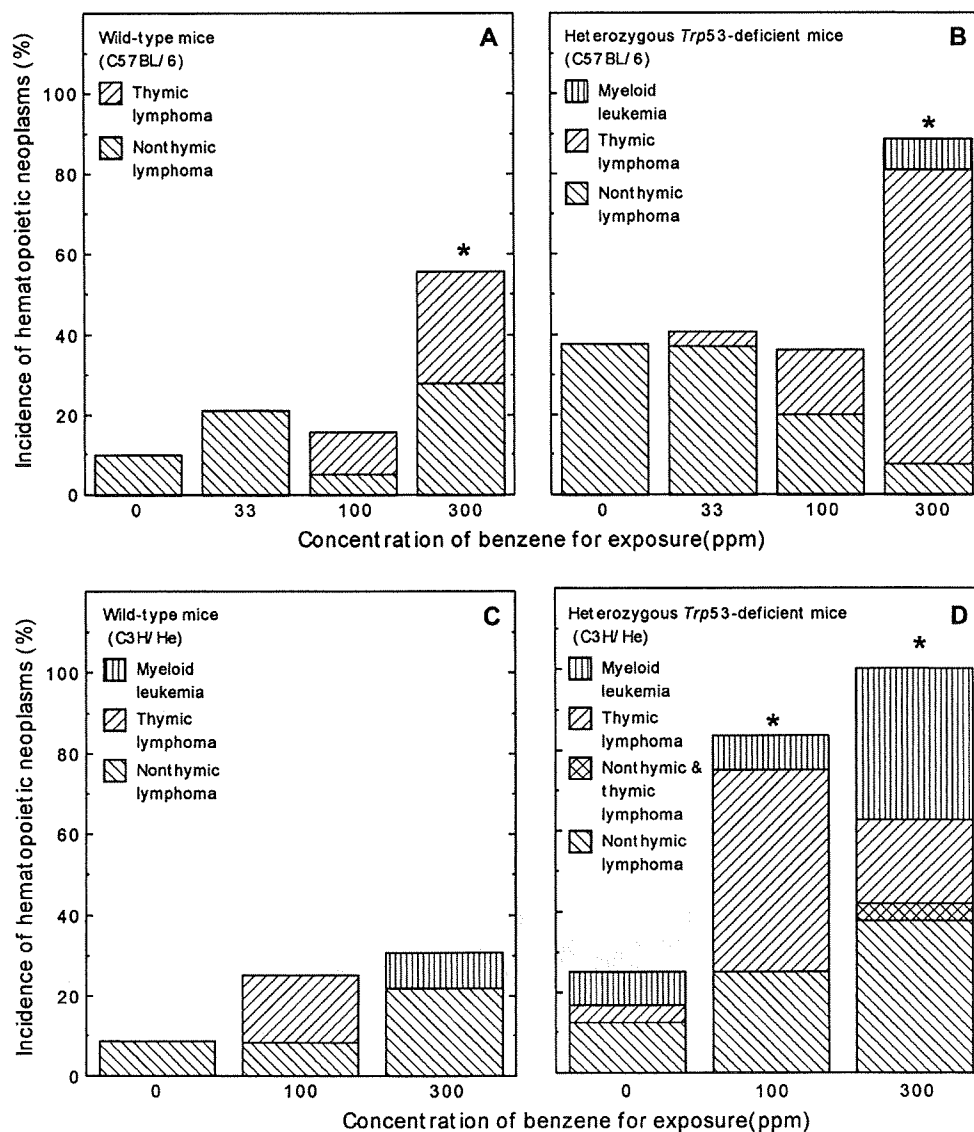


**FIG. 8.** Incidences of HPN histological types are shown in bar graphs. (A, B) C57BL/6 strain, wild-type mice (A) and heterozygous *Trp53*-deficient mice (B); (C, D) C3H/He strain, wild-type mice (C) and heterozygous *Trp53*-deficient mice (D). The incidence of HPNs is shown on the ordinate axis versus benzene exposure dose for the C57BL/6 strain (0, 33, 100, and 300 ppm) or the C3H/He strain (0, 100, and 300 ppm) on the horizontal axis of each graph. Histological types, such as AML, thymic lymphoma, nonthymic lymphoma associated with thymic lymphoma, and nonthymic lymphoma, are designated by inset legends in each figure. Incidences in heterozygous *Trp53*-deficient mice are higher than those in wild-type mice. Incidences in the 300-ppm exposure only (\*) show statistically significant differences for both wild-type mice and heterozygous *Trp53*-deficient mice.

of hematopoietic stem/progenitor cells does not induce any hematopoietic neoplastic growth but rather induces irreversible aplastic anemia (Cronkite *et al.*, 1982). The Snyder-Cronkite benzene exposure protocol of 300 ppm, 6 h/day, 5 days/week, for the animal's lifetime or 16 weeks was originally aimed to not exhaust but maintain hematopoietic stem/progenitor cells. The exposure period was subsequently extended for the protocols up to 2 years in length (Huff *et al.*, 1989; NTP, 1986), but no substantial increase in the incidence of observed

HPNs was reported. The exposure period applied in the present study was longer than in the original protocol by Cronkite *et al.* (1984, 1985, 1989) (16 weeks), which produced a higher incidence of HPNs owing to less exhaustion of hematopoietic stem/progenitor cells even in wild-type mice in both C57BL/6 and C3H/He strains. The relationship between the incidence of HPNs and the benzene exposure dose, however, showed a maximum increase to plateau with benzene exposure at less than 300 ppm (Figs. 2A and 2D). It, thus, appears that the

number of stem/progenitor cells available for targeting at 300 ppm in C3H/He mice is practically marginal not only for thymic lymphomas but also for all HPNs.

The potential for inducing HPNs seems to be limited in wild-type mice, as shown by the present protocol in both C57BL/6 and C3H/He strains as well as in reports by Huff *et al.* (1989) and the NTP (1986). However, we noted enhanced induction of HPNs after benzene exposure in *Trp53*-deficient mice and attributed this to arrest of the stem cell-specific cell cycle possibly owing to the genotoxicity induced by benzene exposure. Moreover, owing to *Trp53* deficiency, benzene exposure in excess of 300 ppm appears to suppress the induction of HPNs as evidenced by the incidence of thymic lymphomas in heterozygous *Trp53*-deficient mice (Fig. 8D). A nonlinear limited increase and plateaued increase in the incidence of HPNs were also confirmed for the higher incidence of HPNs in *Trp53*-deficient mice with an impaired repair system. Regarding the known association between lower benzene toxicity and higher LD<sub>50</sub> values, the results imply a trend based on the possible loss of progenitor cell-specific target cells for HPNs, that is, hematopoietic progenitor cells at higher benzene exposures (Yoon *et al.*, 2002).

*Trp53*-deficient mice develop undifferentiated immature HPNs (Yoshida *et al.*, 2002), which are attributed to the failure of *Trp53* expression to regulate the differentiation process in myeloid cells (Feinstein *et al.*, 1992; Kastan *et al.*, 1991; Skorski *et al.*, 1996; Soddu *et al.*, 1994). As reported previously for radiation-induced AML in *Trp53*-deficient mice (Yoshida *et al.*, 2002, 2007), such AML tends to be characterized by a high incidence of stem cell leukemias and/or blastic leukemias, and there are traces of myeloid differentiation in homozygous *Trp53*-deficient mice with or without radiation exposure. Interestingly, the leukemia developing in *Trp53*-deficient mice after benzene exposure also showed less differentiation in the present study. Such reductions in differentiation are not seen in other thymic or nonthymic lymphomas. However, we were unable to confirm those findings here owing to insufficient data analysis of the precise level of differentiation since differentiation biomarkers for thymic and nonthymic lymphomas were not applied in the present study.

Third, the last issue is why benzene-induced HPNs are not leukemic, but largely thymic and nonthymic lymphomatous in mice (Cronkite *et al.*, 1985; Huff *et al.*, 1989), whereas most of the HPNs that develop after benzene exposure in humans are AMLs (Aksoy *et al.*, 1974; Delore and Borgomano, 1928; Vigliani and Forni, 1976). This query relating to the experimental development of leukemias in the narrow exposure dose range of benzene-induced HPNs has not been satisfactorily answered to date. In the present study, we found a marked difference between C57BL/6 and C3H/He mice in the incidence of different types of HPNs. Specifically, thymic lymphomas were predominantly induced in C57BL/6 mice, whereas nonthymic lymphomas were predominantly induced in C3H/He mice. Our findings may be supported by the gene expression differences

reported for these strains after benzene exposure since the gene expression profiles in both strains were, to some extent, reciprocal for some cell cycle-regulating genes (data not shown). Comparable differences were also observed in the incidence of AMLs. Similar to findings following radiation exposure, C3H/He mice, which are prone to developing AMLs, tended to develop AMLs following benzene exposure.

An exposure-dependent limited increase was again observed in the incidence of AMLs up to 37.5% in *Trp53*-deficient C3H/He mice, and AMLs also developed even in wild-type C3H/He mice when exposed to 300 ppm. However, only two *Trp53*-deficient C57BL/6 mice developed AML at 300 ppm. This implies that there is a potential leukemogenicity not only in the C3H/He strain but also in the C57BL/6 strain, although in the C3H/He strain such leukemogenicity is associated more with an as-yet-undefined genetic background for induction of AMLs.

We noted a few C57BL/6 mice with myeloproliferative and/or myelodysplastic syndrome in the 33-ppm exposure group. This suggests that the protocol of 33-ppm exposure was insufficient for inducing HPNs since these syndromes are considered to be a preleukemic hematopoietic disorder.

#### FUNDING

Grants-in-Aid for Scientific Research C (15510064 and 18510066); the Ministry of Health, Labor and Welfare, Japan—Research Fund (H19-Chemistry 003); National Institute of Health Sciences.

#### ACKNOWLEDGMENTS

We thank Ms E. Tachihara, Mr K. Terasaka, Ms Y. Kondo, Ms C. Aoyagi, Ms Y. Usami, Ms Y. Shinzawa, and Ms M. Uchiyama for excellent technical assistance; Ms Y. Kikuchi, M. Yoshizawa, and Ms M. Hojo for secretarial assistance; and Ms Lee Seaman of Seaman Medical, Inc., for her lucid technical editing and advice.

#### REFERENCES

- Aksoy, M., Erdem, S., and DinCol, G. (1974). Leukemia in shoe-workers exposed chronically to benzene. *Blood* **44**, 837–841.
- Cabot, R. C. (1927). Case 13321 bleeding from the gums. *Boston M. & S.J.* **197**, 236.
- Cronkite, E. P., Bullis, J., Inoue, T., and Drew, R. T. (1984). Benzene inhalation produces leukemia in mice. *Toxicol. Appl. Pharmacol.* **75**, 358–361.
- Cronkite, E. P., Drew, R. T., Inoue, T., and Bullis, J. E. (1985). Benzene hematotoxicity and leukemogenesis. *Am. J. Ind. Med.* **7**, 447–456.
- Cronkite, E. P., Drew, R. T., Inoue, T., Hirabayashi, Y., and Bullis, J. E. (1989). Hematotoxicity and carcinogenicity of inhaled benzene. *Environ. Health Perspect.* **82**, 97–108.
- Cronkite, E. P., Inoue, T., Carsten, A. L., Miller, M. E., Bullis, J. E., and Drew, R. T. (1982). Effects of benzene inhalation on murine pluripotent stem cells. *J. Toxicol. Environ. Health* **9**, 411–421.

- Delore, P., and Borgomano, C. (1928). Leucémie aiguë au cours de l'intoxication benzénique. Sur l'origine toxique de certaines leucémies aiguës et leurs relations avec les anémies graves. *J. de méd de Lyon* **9**, 227–233.
- Feinstein, E., Gale, R. P., Reed, J., and Canaani, E. (1992). Expression of the normal p53 gene induces differentiation of K562 cells. *Oncogene* **7**, 1853–1857.
- French, J. E., Lacks, G. D., Trempus, C., Dunnick, J. K., Foley, J., Mahler, J., Tice, R. R., and Tennant, R. W. (2001). Loss of heterozygosity frequency at the Trp53 locus in p53-deficient (+/-) mouse tumors is carcinogen- and tissue-dependent. *Carcinogenesis* **22**, 99–106.
- Frith, C. H., Ward, J. M., Harleman, J. H., Stromberg, P. C., Halm, S., Inoue, T., and Wright, J. A. (2001). Hematopoietic system. In *International Classification of Rodent Tumors: The Mouse* (U. Mohr, Ed.), pp. 417–451. Springer-Verlag Berlin, Heidelberg, Berlin.
- Haines, B. B., Ryu, C. J., Chang, S., Protopopov, A., Luch, A., Kang, Y. H., Draganov, D. D., Fragoso, M. F., Paik, S. G., Hong, H. J., et al. (2006). Block of T cell development in P53-deficient mice accelerates development of lymphomas with characteristic RAG-dependent cytogenetic alterations. *Cancer Cell* **9**, 109–120.
- Harvey, M., McArthur, M. J., Montgomery, C. A., Jr., Butel, J. S., Bradley, A., and Donehower, L. A. (1993). Spontaneous and carcinogen-induced tumorigenesis in p53-deficient mice. *Nat. Genet.* **5**, 225–229.
- Hirabayashi, Y., Inoue, T., Suda, Y., Aizawa, S., Ikawa, Y., and Kanisawa, M. (1992). Hemopoietic neoplasms in lethally irradiated mice repopulated with bone marrow cells carrying the human c-myc oncogene: A repopulation assay. *Exp. Hematol.* **20**, 167–172.
- Hirabayashi, Y., Matsuda, M., Aizawa, S., Kodama, Y., Kanno, J., and Inoue, T. (2002). Serial transplantation of p53-deficient hemopoietic progenitor cells to assess their infinite growth potential. *Exp. Biol. Med. (Maywood)* **227**, 474–479.
- Hirabayashi, Y., Yoshida, K., Aizawa, S., Kodama, Y., Kanno, J., Kurokawa, Y., Yoshimura, I., and Inoue, T. (2003). Evaluation of nonthreshold leukemogenic response to methyl nitrosourea in p53-deficient C3H/He mice. *Toxicol. Appl. Pharmacol.* **190**, 251–261.
- Huff, J. E., Haseman, J. K., DeMarini, D. M., Eustis, S., Maronpot, R. R., Peters, A. C., Persing, R. L., Chrisp, C. E., and Jacobs, A. C. (1989). Multiple-site carcinogenicity of benzene in Fischer 344 rats and B6C3F1 mice. *Environ. Health Perspect.* **82**, 125–163.
- Kastan, M. B., Radin, A. I., Kuerbitz, S. J., Onyekwere, O., Wolkow, C. A., Civin, C. I., Stone, K. D., Woo, T., Ravindranath, Y., and Craig, R. W. (1991). Levels of p53 protein increase with maturation in human hematopoietic cells. *Cancer Res.* **51**, 4279–4286.
- Kemp, C. J., Wheldon, T., and Balmain, A. (1994). p53-deficient mice are extremely susceptible to radiation-induced tumorigenesis. *Nat. Genet.* **8**, 66–69.
- Lan, Q., Zhang, L., Li, G., Vermeulen, R., Weinberg, R. S., Dosemeci, M., Rappaport, S. M., Shen, M., Alter, B. P., Wu, Y., et al. (2004). Hematotoxicity in workers exposed to low levels of benzene. *Science* **306**, 1774–1776.
- Le Noir, M. M., and Claude, H. (1897). Sur un cas de purpura attribué à l'intoxication par la benzine. *Bull. Med. Soc. Hop. Paris* **14**, 1251–1260.
- Li, G. X., Hirabayashi, Y., Yoon, B. I., Kawasaki, Y., Tsuboi, I., Kodama, Y., Kurokawa, Y., Yodoi, J., Kanno, J., and Inoue, T. (2006). Thioredoxin overexpression in mice, model of attenuation of oxidative stress, prevents benzene-induced hemato-lymphoid toxicity and thymic lymphoma. *Exp. Hematol.* **34**, 1687–1697.
- MacDonald, J., French, J. E., Gerson, R. J., Goodman, J., Inoue, T., Jacobs, A., Kasper, P., Keller, D., Lavin, A., Long, G., et al. (2004). The utility of genetically modified mouse assays for identifying human carcinogens: A basic understanding and path forward. The Alternatives to Carcinogenicity Testing Committee ILSI HESI. *Toxicol. Sci.* **77**, 188–194.
- Maltoni, C., Ciliberti, A., Cotti, G., Conti, B., and Belpoggi, F. (1989). Benzene, an experimental multipotential carcinogen: Results of the long-term bioassays performed at the Bologna Institute of Oncology. *Environ. Health Perspect.* **82**, 109–124.
- Mouse Genome Informatics. (2009). *Trp53tm1Sia Targeted Allele Detail, ID: MGI: 1926340* Available at: <http://www.informatics.jax.org/javawi2/servlet/WIFetch?page=alleleDetail&key=2871>. Accessed June 4, 2009.
- NTP. (1986). Toxicology and carcinogenesis studies of benzene (CAS No. 71-43-2) in F344/N rats and B6C3F1 mice (Gavage Studies). *Natl. Toxicol. Program Tech. Rep. Ser.* **289**, 1–277.
- Penati, F., and Vigliani, E. C. (1938). Sul problema delle mielopatie aplastiche pseudoaplastiche e leucemiche d benzolo. *Ras. Med. Ind.* **9**, 345–361.
- Santesson, C. G. (1897). Über chronische Vergiftungen mit Steinkohlenteerbenzin: vier Todesfälle. *Arch. Hyg. Berl.* **31**, 336–376.
- Seki, M., Yoshida, K., Nishimura, M., and Nemoto, K. (1991). Radiation-induced myeloid leukemia in C3H/He mice and the effect of prednisolone acetate on leukemogenesis. *Radiat. Res.* **127**, 146–149.
- Selling, L. (1910). A preliminary report on some cases of purpura haemorrhagica due to benzol poisoning. *Bull. Johns Hopkins Hosp.* **21**, 33–37.
- Skorski, T., Nieborowska-Skorska, M., Wlodarski, P., Perrotti, D., Martinez, R., Wasik, M. A., and Calabretta, B. (1996). Blastic transformation of p53-deficient bone marrow cells by p210bcr/abl tyrosine kinase. *Proc. Natl. Acad. Sci. U. S. A.* **93**, 13137–13142.
- Smith, A. R. (1928). Chronic benzol poisoning among women industrial workers: A study of the women exposed to benzol fumes in six factories. *J. Indust. Hyg.* **10**, 73–93.
- Snyder, C. A., Goldstein, B. D., Sellakumar, A. R., Bromberg, I., Laskin, S., and Albert, R. E. (1980). The inhalation toxicology of benzene: Incidence of hematopoietic neoplasms and hematotoxicity in ARK/J and C57BL/6J mice. *Toxicol. Appl. Pharmacol.* **54**, 323–331.
- Snyder, R. (2002). Benzene and leukemia. *Crit. Rev. Toxicol.* **32**, 155–210.
- Snyder, R. (2007). Benzene's toxicity: A consolidated short review of human and animal studies by HA Khan. *Hum. Exp. Toxicol.* **26**, 687–696.
- Soddu, S., Blandino, G., Citro, G., Scardigli, R., Piaggio, G., Ferber, A., Calabretta, B., and Sacchi, A. (1994). Wild-type p53 gene expression induces granulocytic differentiation of HL-60 cells. *Blood* **83**, 2230–2237.
- Storer, R. D., French, J. E., Haseman, J., Hajian, G., LeGrand, E. K., Long, G. G., Mixson, L. A., Ochoa, R., Sagartz, J. E., and Soper, K. A. (2001). P53<sup>+/-</sup> hemizygous knockout mouse: Overview of available data. *Toxicol. Pathol.* **29**(Suppl), 30–50.
- Tsukada, T., Tomooka, Y., Takai, S., Ueda, Y., Nishikawa, S., Yagi, T., Tokunaga, T., Takeda, N., Suda, Y., Abe, S., et al. (1993). Enhanced proliferative potential in culture of cells from p53-deficient mice. *Oncogene* **8**, 3313–3322.
- Vigliani, E. C., and Forni, A. (1976). Benzene and leukemia. *Environ. Res.* **11**, 122–127.
- WHO. (2003). *Benzene in Drinking-Water. Background Document for Development of WHO Guidelines for Drinking-Water Quality*. WHO/SDE/WSH/03.04/24. Accessed June 4, 2009. Originally published in *Guidelines for drinking-water quality, 2nd ed. Vol. 2. Health criteria and other supporting information*. World Health Organization, Geneva.
- Yagi, T., Tokunaga, T., Furuta, Y., Nada, S., Yoshida, M., Tsukada, T., Saga, Y., Takeda, N., Ikawa, Y., and Aizawa, S. (1993). A novel ES cell line, TT2, with high germline-differentiating potency. *Anal. Biochem.* **214**, 70–76.
- Yoon, B. I., Hirabayashi, Y., Kawasaki, Y., Kodama, Y., Kaneko, T., Kanno, J., Kim, D. Y., Fujii-Kuriyama, Y., and Inoue, T. (2002). Aryl hydrocarbon receptor mediates benzene-induced hematotoxicity. *Toxicol. Sci.* **70**, 150–156.
- Yoon, B. I., Hirabayashi, Y., Kawasaki, Y., Kodama, Y., Kaneko, T., Kim, D. Y., and Inoue, T. (2001). Mechanism of action of benzene toxicity: Cell cycle suppression in hemopoietic progenitor cells (CFU-GM). *Exp. Hematol.* **29**, 278–285.

- Yoon, B. I., Li, G. X., Kitada, K., Kawasaki, Y., Igarashi, K., Kodama, Y., Inoue, T., Kobayashi, K., Kanno, J., Kim, D. Y., *et al.* (2003). Mechanisms of benzene-induced hematotoxicity and leukemogenicity: cDNA microarray analyses using mouse bone marrow tissue. *Environ. Health Perspect.* **111**, 1411–1420.
- Yoshida, K., Aizawa, S., Watanabe, K., Hirabayashi, Y., and Inoue, T. (2002). Stem-cell leukemia: p53 deficiency mediated suppression of leukemic differentiation in C3H/He myeloid leukemia. *Leuk. Res.* **26**, 1085–1092.
- Yoshida, K., Hirabayashi, Y., Wada, S., Watanabe, F., Watanabe, K., Aizawa, S., and Inoue, T. (2007). p53 (TRP53) deficiency-mediated antiapoptosis escape after 5 Gy X irradiation still induces stem cell leukemia in C3H/He mice: Comparison between whole-body assay and bone marrow transplantation (BMT) assay. *Radiat. Res.* **167**, 703–710.
- Yoshida, K., Nojima, K., Seki, M., and Inoue, T. (1996). Radiation-induced myeloid leukemia following splenectomy in C3H/He mice. *J. Radiat. Res.* **37**, 380.

## Benzene activates caspase-4 and -12 at the transcription level, without an association with apoptosis, in mouse bone marrow cells lacking the p53 gene

Jung-Yeon Yi · Yoko Hirabayashi · Yang-Kyu Choi ·  
Yukio Kodama · Jun Kanno · Jeong-Hee Han ·  
Tohru Inoue · Byung-Il Yoon

Received: 11 November 2008 / Accepted: 10 March 2009 / Published online: 27 March 2009  
© Springer-Verlag 2009

**Abstract** Benzene is a well-known environmental pollutant that can induce hematotoxicity, aplastic anemia, acute myelogenous leukemia, and lymphoma. However, although benzene metabolites are known to induce oxidative stress and disrupt the cell cycle, the mechanism underlying lympho/leukemogenicity is not fully understood. Caspase-4 (alias caspase-11) and -12 are inflammatory caspases implicated in inflammation and endoplasmic reticulum stress-induced apoptosis. The objectives of this study were to investigate the altered expression of caspase-4 and -12 in mouse bone marrow after benzene exposure and to determine whether their alterations are associated with benzene-induced bone marrow toxicity, especially cellular apoptosis. In addition, we evaluated whether the p53 gene is involved in regulating the mechanism, using both wild-type (WT) mice and mice lacking the p53 gene. For this study, 8-week-old C57BL/6 mice [WT and p53 knockout (KO)] were administered a benzene solution (150 mg/kg diluted in

corn oil) via oral gavage once daily, 5 days/week, for 1 or 2 weeks. Blood and bone marrow cells were collected and cell counts were measured using a Coulter counter. Total mRNA and protein extracts were prepared from the harvested bone marrow cells. Then qRT-PCR and Western blotting were performed to detect changes in the caspases at the mRNA and protein level, respectively. A DNA fragmentation assay and Annexin-V staining were carried out on the bone marrow cells to detect apoptosis. Results indicated that when compared to the control, leukocyte number and bone marrow cellularity decreased significantly in WT mice. The expression of caspase-4 and -12 mRNA increased significantly after 12 days of benzene treatment in the bone marrow cells of benzene-exposed p53KO mice. However, apoptosis detection assays indicated no evidence of apoptosis in p53KO or WT mice. In addition, no changes of other apoptosis-related caspases, such as caspase-3 and -9, were found in WT or p53KO mice at the level of mRNA and proteins. These results indicated that upregulation of caspase-4 and -12 in mice lacking the p53 gene is not associated with cellular apoptosis. In conclusion, caspase-4 and -12 can be activated by benzene treatment without inducing cell apoptosis in mouse bone marrow, which are partly under the regulation of the p53 gene.

J.-Y. Yi and Y. Hirabayashi contributed equally for this study.

J.-Y. Yi · J.-H. Han · B.-I. Yoon (✉)  
School of Veterinary Medicine, Kangwon National University,  
192-1 Hyoja 2, Chuncheon, Gangwon 200-701, Republic of Korea  
e-mail: byoon@kangwon.ac.kr

Y. Hirabayashi · Y. Kodama · J. Kanno  
Division of Cellular and Molecular Toxicology,  
Center for Biological Safety and Research,  
National Institute of Health Sciences, Tokyo, Japan

Y.-K. Choi  
College of Veterinary Medicine, Konkuk University,  
Seoul, Republic of Korea

T. Inoue  
Biological Safety and Research Center,  
National Institute of Health Sciences, Tokyo, Japan

**Keywords** Apoptosis · Benzene · Bone marrow ·  
Caspase-4 · Caspase-12 · Mouse, p53

### Introduction

Benzene is a well-known environmental pollutant found in gasoline, automobile exhaust, and cigarette smoke (Lyngge et al. 1997; Rana and Verma 2005; Wallace 1996). Exposure to benzene is associated with hematotoxicity, which

may give rise to aplastic anemia, acute myelogenous leukemia, and lymphoma (Brief et al. 1980; Cronkite 1986; Farris et al. 1997; Huff et al. 1989; Rinsky et al. 1981; Snyder et al. 1980; Snyder et al. 1988). Furthermore, benzene has been postulated to have multisite carcinogenicity because it leads to tumor development in various organs such as lung, oral cavity, Harderian gland, mammary gland, and skin (Huff et al. 1989; Maltoni et al. 1989; Snyder et al. 1988). Once absorbed, benzene is metabolized into a variety of intermediate compounds, including benzene oxide, phenol, catechol, hydroquinone, and benzoquinone. This conversion occurs in several organs, including the liver and bone marrow (Snyder and Hedli 1996). Phenol metabolites derived from benzene oxide via cytochrome P450 2E1 (CYP2E1) (Ross 2000) are believed to generate reactive oxygen species (ROS) after hydroxylation by myeloperoxidase. Once the oxidative aggression surpasses the antioxidant defense system in cells, the resultant oxidative stress can induce hematology toxicity in bone marrow (Hiraku and Kawanishi 1996; Kuo et al. 1999). However, the mechanism underlying lympho/leukemogenicity is not fully understood, although benzene metabolites are known to induce oxidative stress and disrupt the cell cycle (Danial and Korsmeyer 2004; Rao and Snyder 1995; Yoon et al. 2001).

Caspase-4 and -12 are inflammatory caspases, characterized by the presence of a large prodomain containing a typical caspase recruitment domain (CARD) at the N-terminus (Martinon and Tschoop 2007). Caspase-4 is proinflammatory in that it activates caspase-1, while caspase-12 is considered to function as a negative regulator of the inflammatory signaling pathway (Lamkanfi et al. 2007). However, their precise functions and regulatory mechanisms remain elusive. In addition to the implications of the caspases in inflammation, they are also thought to be involved in apoptosis of specific cell populations, such as nerve cells (Fan et al. 2005; Hisahara et al. 2001; Kang et al. 2000; Scott and Saleh 2007; Suk et al. 2002). According to previous studies, activation of caspase-4 and -12 is mediated via both p53-dependent and -independent pathways, depending on the pathogenic situation (Choi et al. 2001; Fábíán et al. 2007), but their alterations and possible roles have not been studied in association with the underlying mechanisms of benzene toxicity. Recently, microarray analyses indicated that caspase-4 can be activated in benzene-exposed mouse bone marrow (Yoon et al. 2003), suggesting that they could play some roles in the action mechanisms of benzene in the bone marrow, via either p53-mediated or independent mechanisms.

Thus, in the present study, we investigated the altered expression of caspase-4 and -12 in the mouse bone marrow following benzene exposure and explored whether their alterations are associated with benzene-induced bone

marrow toxicity, especially cellular apoptosis. Furthermore, we evaluated whether the p53 gene is implicated in regulating the mechanism using both wild-type (WT) mice and mice lacking the p53 gene.

## Materials and methods

### Animals

The targeting vector for the *Trp53* gene, a 2.8-kb recombinant plasmid containing a neomycin-resistant gene just before the transcriptional starting site, was inserted into TT2 embryonic stem cells (heterozygous for C57BL/6 and CBA; Yagi et al. 1993) to establish the homologous recombinant clones (Tsukada et al. 1993). By means of an aggregation chimera with the recombinant clones, chimeric mice were produced, followed by establishing *Trp53*-knockout mice in 1987 after confirmation of the germinal transmission of *Trp53*-deficient (C57BL/6 × CBA) F1 mice (Tsukada et al. 1993). General information about the recombinant mice is also available elsewhere (*Trp53*<sup>tm1Sia</sup> MGI: 1926340, Mouse Genome Informatics 2009). The original *Trp53*-deficient (C57BL/6 × CBA) F1 mice crossed back into C57BL/6 were transferred to the animal facility of the National Institute of Health Sciences (NIHS, Tokyo, Japan) at the second generation. Backcrossing into C57BL/6 occurred over 20 generations in 1997 and their backcrossing has been continuously maintained.

In this study, male WT and homozygous *Trp53*-deficient mice were used. The homozygous *Trp53*-deficient mice and WT mice were generated by mating between heterozygous *Trp53*-deficient mice at the animal facility of the NIHS. Neonates were genotyped by primer for the targeted DNA sequence, including a partial *neo* gene on the 5' side of exon 4 by polymerase chain reaction (PCR) analysis using tissue obtained from the tail (Hirabayashi et al. 2002; Tsukada et al. 1993; Yoshida et al. 2002). Genotyping was conducted using five 8-week-old mice for each genotype. During the study, the mice were kept on a 12-h light–dark cycle, an autoclave-sterilized basal pellet diet (CRF-1; Oriental Yeast Co., Ltd., Tokyo, Japan) and distilled water were provided ad libitum throughout the study. Temperature and humidity were maintained automatically at  $24 \pm 1^\circ\text{C}$  and  $55 \pm 10\%$ , respectively.

All animals were maintained in the board-approved laboratory animal facility of the NIHS. All experimental protocols involving the laboratory mice used in this study were reviewed by the Interdisciplinary Monitoring Committee for the Proper Animal Use and Welfare of Experimental Animals (ICRAW), a peer reviewed panel established at the NIHS, and approved by the Committee for Animal Care and Use (CACU) of the NIHS and the Institutional Animal

Care and Use Committee (IACUC) at Kangwon National University for compliance with the National Research Council's Guide for the Care and Use of Laboratory Animals (NRC 1996). All animal studies were conducted using humane protocols approved by the CACU and Kangwon National University.

#### Benzene exposure

Benzene (CAS No. 319953; Sigma-Aldrich, St. Louis, MO, USA) was diluted in corn oil (CAS No. C8267; Sigma-Aldrich) and administered via oral gavage in a single dose of 150 mg/kg in a volume of 10 ml/kg b.w. once daily, 5 days/week, for 1 or 2 weeks; this protocol was shown to create an effect on mouse bone marrow similar in grade to the effect produced when 300 ppm benzene is inhaled (Yi and Yoon 2008). The sham control groups were administered corn oil (Sigma-Aldrich) alone during the same period. The mice were killed 2 h after the last treatment; and peripheral blood and bone marrow cells were then harvested. The experimental schedules for sham and benzene-treated mice are shown in Fig. 1. Five mice per group were used for each experiment.

#### Peripheral blood and bone marrow harvesting

Blood and bone marrow cells were collected from the orbital sinus and both femora of each mouse, respectively; then peripheral blood and bone marrow cell counts were performed using a blood cell counter (Sysmex K-4500; Sysmex, Tokyo, Japan).

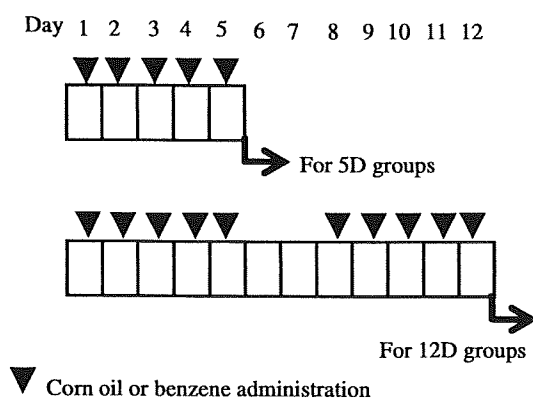


**Fig. 1** Experimental protocol. Benzene (150 mg/kg) or vehicle alone (corn oil) was administered by oral gavage once daily, 5 days/week, for 1 or 2 weeks. The mice were killed 4 h after the final treatment on day 5 or day 12 and bone marrow cells were harvested from both femora of each individual

#### Collection of bone marrow cells

Bone marrow cells were harvested from both femora of each mouse. Bone marrow cells were flushed out of the bone shaft using a 27-gauge hypodermic needle filled with 2 ml of Dulbecco's modified minimum Eagle's medium (DMEM) without phenol red (Invitrogen, Carlsbad, CA, USA). The bone marrow cells were then passed repeatedly through a needle to produce a single-cell suspension. After lysis of red blood cells, a portion of the bone marrow cells was subjected to total RNA extraction using TRIzol reagent (Invitrogen), and the remaining cells were frozen in liquid nitrogen and stored at  $-80^{\circ}\text{C}$  until required for Western blotting or DNA fragmentation analysis.

#### PCR for genotyping

To detect *Trp53* WT and *Trp53*-deficient alleles, PCR was performed using genomic DNA extracted from the tail of each mouse, and synthetic oligonucleotides were used as primers as described elsewhere (Tsukada et al. 1993). Briefly to detect the *Trp53* WT allele, the 5' common primer (5'-aattgacaagttatgcatcca-3') and the 3' primer (5'-actcctcaacatcctggggcagcaacagat-3) were used; to detect the *Trp53*-deficient allele, the 5' common primer and *neo* sequence primer (5'-gaacctgcgtgcaatccatctgttcaatg-3') were used.

#### Annexin-V staining

Bone marrow cells harvested from vehicle- and benzene-treated mice were suspended in an annexin-V-fluorescein isothiocyanate (FITC) binding buffer at a final concentration of  $1 \times 10^6$  cells/ml. Annexin-V staining was performed according to the manufacturer's protocol and quantified using a flow cytometer (Beckman-Coulter, Miami, FL, USA).

#### DNA fragmentation assay

To detect DNA fragmentation in bone marrow cells, DNA laddering assays were performed using a commercially available kit (Roche, Mannheim, Germany) according to the manufacturer's protocol. Briefly, the harvested bone marrow cells were mixed with 180  $\mu\text{l}$  of phosphate-buffered saline (PBS) and 200  $\mu\text{l}$  of binding/lysis buffer. The suspensions were incubated for 10 min at room temperature and then shaken after adding 100  $\mu\text{l}$  of isopropanol. The samples were pipetted into the upper reservoir of a combined filter and collection tube, and then centrifuged for 1 min at 8,000 rpm. After discarding the flow-through solution, 500  $\mu\text{l}$  of washing buffer was added to the upper reservoir and the tube was centrifuged again for 1 min at 8,000 rpm.



This process was repeated twice. Finally, the residual washing buffer was removed and the DNA was eluted. The purified DNA was run through an agarose gel and DNA fragments were visualized under a UV light source and photographed.

#### Preparation of total RNA

Total RNA was extracted from the harvested bone marrow cells using TRIzol reagent (Invitrogen) according to the manufacturer's instructions. Briefly, the harvested cells were mixed with TRIzol reagent, pipetted repeatedly, and then incubated for 5 min at room temperature to permit complete dissociation of nucleoprotein complexes. After incubation, 0.2 ml of chloroform was added to the suspensions, followed by vigorous shaking for 15 s and further incubation at room temperature for 3 min. The samples were then centrifuged at 14,000 rpm for 15 min at 4°C. The aqueous phase was precipitated by mixing with 0.5 ml of isopropyl alcohol, followed by centrifugation at 14,000 rpm for 10 min at 4°C. After centrifugation, the supernatant was removed and the RNA pellet was washed once in 1 ml of 75% ethanol. The pellet was then dried and dissolved in RNA-free water.

#### qRT-PCR analysis of caspase-4, -12 and other apoptosis-related genes

We examined the mRNA expression of caspase-4 and 12 and other apoptosis-related genes, caspase-3, caspase-9, Smad6 and Bcl2, using TaqMan RT-PCR with an ABI 7900 system (Applied Biosystems, Foster City, CA, USA). The reaction mixtures were incubated at 50°C for 2 min and 95°C for 10 min, followed by 40 cycles of PCR amplification at 95°C for 15 s and at 60°C for 1 min. Gene-specific probes and primer pairs for caspase-4 (Gene ID: Mm00432307\_m1), caspase-12 (Gene ID: Mm00438038), caspase-3 (Mm00438045), caspase-9 (Gene ID: Mm00516563\_m1), Bcl2 (Gene ID: Mm00477631\_m1) and Smad6 (Gene ID: Mm00484738\_m1) were used. For each probe/primer set a standard curve was generated which was used to confirm that the number of transcripts increased linearly with increasing amounts of cDNA. Benzene-induced alterations in gene expression in comparison to the control group were calculated using the comparative Ct method. As an internal control the results were expressed relative to the quantity of GAPDH transcripts.

#### Western blot assays for caspase-4, -12 and other apoptosis-related proteins

Protein extracts were prepared from harvested bone marrow cells using protein extraction buffer purchased from

iNtRON (cat. no. 17081; Chinju, Korea) according to the manufacturer's instructions. Briefly, pellets of frozen bone marrow cells were suspended in 500 µl of protein extraction buffer using a 26-gauge syringe. After incubation for 15 min at -20°C, the suspension was centrifuged at 13,000 rpm for 5 min at 4°C. Following centrifugation, the supernatant was transferred to a fresh tube and protein content was quantified using a bicinchoninic acid (BCA) solution (cat. no. B9643; Sigma-Aldrich) and a spectrophotometer (Beckman Instruments, Fullerton, CA, USA). The protein extracts (10 µg) were denatured, subjected to 12% (w/v) SDS-polyacrylamide gel electrophoresis (PAGE), and then transferred to a polyvinylidene fluoride (PVDF) membrane (Bio-Rad, Hercules, CA, USA). After blocking nonspecific binding sites by incubating the membranes in 5% nonfat dried milk and 0.1% Tween 20 in Tris-buffered saline (TTBS, pH 7.4) for 1 h at room temperature, the membranes were incubated overnight at 4°C in the presence of the appropriate diluted primary antibodies (Santa Cruz Biotechnology, Santa Cruz, CA, USA); rabbit polyclonal antibodies were used for caspase-4 (epitope corresponding to amino acids 301–350 of murine caspase-11), -12 (epitope corresponding to amino acids 38–145 mapping near the N-terminus of murine caspase-12), caspase-9 (epitope corresponding to amino acids 315–397 mapping within the C-terminus of human caspase-9 with cross reactivity to murine caspase-9), Smad6 (epitope corresponding to amino acids 41–190 mapping near the N-terminus of human Smad6 with cross reactivity to murine Smad6) and Bcl2 (epitope corresponding to amino acids 1–205 of human Bcl2 with cross reactivity to murine Bcl2). After washing in TTBS, the membranes were incubated with diluted horseradish peroxidase-conjugated secondary antibodies (Santa Cruz Biotechnology) for 1 h at room temperature. To visualize the bands, the membranes were treated with a detection reagent (Santa Cruz Biotechnology) for 1 min and then exposed to film.

#### Analysis of the data of qRT-PCR and statistical evaluation

The results of qRT-PCR were processed using the delta Ct method. Statistically significant differences between the treated and control groups were detected using Student's *t* test. Statistical significance was set at  $P < 0.05$  or  $P < 0.01$ .

## Results

#### Changes in peripheral blood and bone marrow cell counts

In WT mice, 5- and 12-day benzene treatments resulted in a considerable decrease in the number of peripheral leukocytes to 70 and 90% of the mean control values, respectively

(Fig. 2a). However, no change was noted in p53KO mice as a result of benzene treatment (Fig. 2b). Bone marrow cellularity significantly decreased to 80.5 and 81.6% of the mean control values in WT mice treated with 150 mg/kg b.w. of benzene for 5 and 12 days, respectively (Fig. 3a). In p53 KO mice, bone marrow cellularity also decreased to 89.3 and 83.3%, respectively, but the difference was not significantly different from that of the control group (Fig. 3b).

#### Expression of caspase-4, caspase-12 and other apoptosis-related genes in bone marrow

Benzene treatment for 5 days appeared to suppress the expression of caspase-3 and -9 in bone marrow cells harvested from WT mice, although the difference was not significant. No changes were noted in the expression of caspase-4, caspase-12, Bcl2 and Smad6 mRNA following the 5-day benzene treatment. After 12 days of benzene treatment, the cell survival genes Bcl2 and Smad6 seemed to be suppressed in response to a 12-day benzene treatment, but no significant difference was noted because of individual variations. The expression of caspase-4, -12, -3 and -9 remained within the control range of mRNA expression in the bone marrow of WT mice (Fig. 4a).

In mice lacking of the p53 gene, however, the mRNA expression level of caspase-4 and -12 were significantly

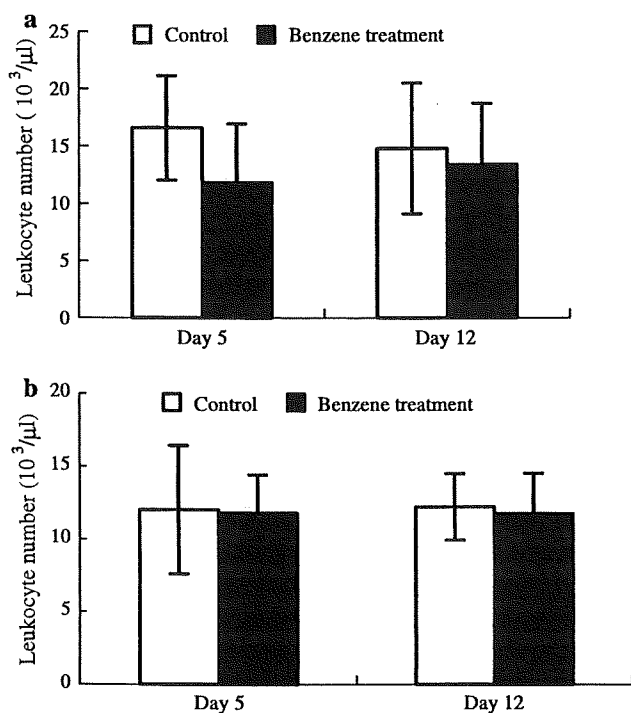


**Fig. 2** Effect of benzene on leukocyte numbers in wild-type (a) and p53 knockout (b) mice treated with 150 mg/kg benzene once daily for 5 or 12 days

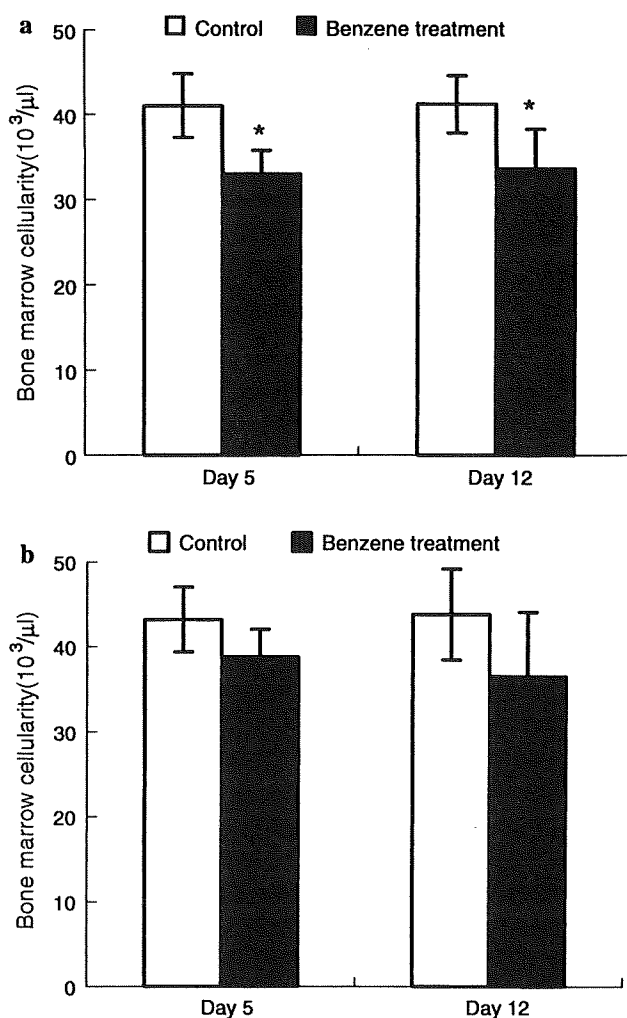


**Fig. 3** Effect of benzene on bone marrow cellularity in wild-type (a) and p53 knockout (b) mice treated with 150 mg/kg benzene once daily for 5 or 12 days

upregulated after 12 days of benzene treatment (Fig. 4b), and although no significant difference was detected, caspase-3 and -9 mRNA levels also showed a tendency to increase after 12 days of treatment (Fig. 4b). In addition, unlike in WT mice, the 5-day benzene treatment induced bcl-2 expression, followed by a return to control levels after 12 days of treatment.

#### Expression of caspase-4, caspase-12 and other apoptosis-related proteins in bone marrow

Caspase-9, -11, and -12 and Bcl2 protein expression did not change or was undetectable in WT and p53KO mice under the conditions used in this study. Smad6 protein expression appeared to increase marginally in benzene-treated WT mice compared to the control, but this difference was not significant (Fig. 5).

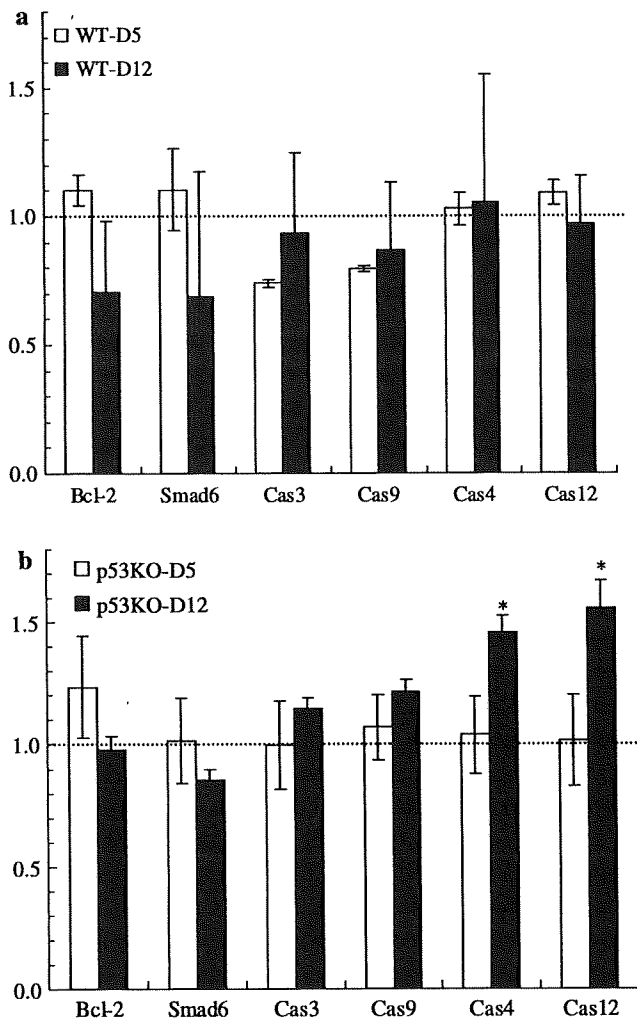


**Fig. 4** Effect of benzene on the expression of apoptosis-associated genes in wild-type (a) and p53 knockout (b) mice. The ratio was determined by dividing the mean value of the treatment group by the mean value of the respective control group. WT-D5 and WT-D12: wild-type mice treated for 5 or 12 days, respectively; p53KO-D5 and p53KO-D12: p53 knockout mice treated for 5 or 12 days, respectively; *Cas* caspase. \*Significantly different compared to the vehicle control at  $P < 0.05$

#### Annexin-V staining and DNA fragmentation assays

Based on the annexin-V staining (Fig. 6) and DNA fragmentation assays (Fig. 7), 5- and 12-day benzene treatments did not induce apoptosis in bone marrow cells harvested from WT or p53KO mice.

#### Discussion

Inflammatory caspases are encoded by three main genes, caspase-1, -4, and -12 in mice (Martinon and Tschopp 2007) which have been postulated to play critical roles in

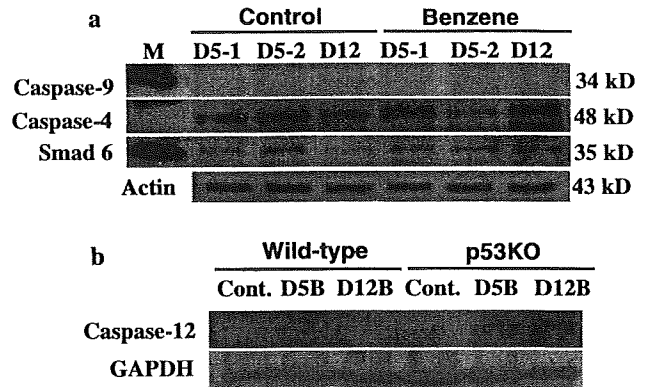


**Fig. 5** Effect of benzene on the expression of selected apoptosis-related proteins. Western blotting revealed no alteration in the expression of caspase-9 or -4 in the benzene-exposed bone marrow cells of wild-type mice (a). Smad6 showed a slight but nonsignificant increase after benzene treatment in the wild-type mice (a). Caspase-12, which is upregulated at the transcriptional level in benzene exposed bone marrow cells of p53KO mice, did not change at the protein level in p53KO mice or wild-type mice (b). D5B and D12B: 150 mg/kg b.w. benzene treatment for 5 and 12 days, respectively. Control mice were administered vehicle corn oil for 5 days (D5) or 12 days (D12)

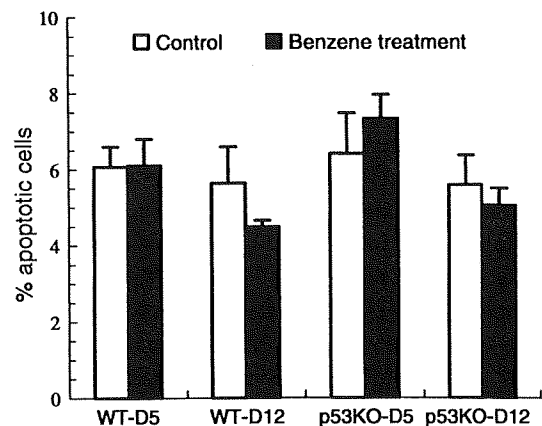


**Fig. 6** Percentage of cells undergoing apoptosis as determined by annexin-V staining. Apoptosis was not detected in mouse bone marrow cells exposed to benzene for up to 12 days. WT-D5 and WT-D12: wild-type mice treated with or without 150 mg/kg benzene for 5 or 12 days, respectively; p53KO-D5 and p53KO-D12: p53 knockout mice treated with or without 150 mg/kg benzene for 5 or 12 days, respectively

inflammation (Martinon and Tschopp 2007; Scott and Saleh 2007). Recently, these inflammatory caspases have gained attention in association with their roles in the induction of apoptosis in specific cell populations, such as macrophages and neuronal cells, represented by endoplasmic reticulum (ER) stress-induced cell death (Fan et al. 2005; Lamkanfi et al. 2007). With regard to the mechanisms of benzene-induced bone marrow toxicity, our previous microarray results indicated some alteration of these



**Fig. 7** DNA laddering assay. DNA fragmentation was not detected in bone marrow cells harvested from wild-type (WT) or p53 knockout (p53KO) mice exposed to benzene. *M* marker; *PC* positive control; *A* WT-5C; *B* WT-5B; *C* WT-12C; *D* WT-12B; *E* p53KO-5C; *F* p53KO-5B; *G* p53KO-12C; *H* p53KO-12B. The animals were treated with vehicle corn oil (5C and 12C) or 150 mg/kg benzene (5B and 12B) for 5 or 12 days, respectively

inflammatory caspases (Yoon et al. 2003), suggesting that they might be implicated in the toxic mechanism of benzene, possibly via induction of bone marrow cell apoptosis. Thus, the objectives of this study were to investigate the altered expressions of the inflammatory caspases as well as apoptosis-activator and -executioner caspases after benzene exposure, and to evaluate whether their alteration is associated with apoptosis. Moreover, by using mice lacking the p53 gene, we assessed the possible role of the p53 gene in the regulation of the inflammatory caspases in mouse bone marrow exposed to benzene.

Consistent with previous studies, benzene administered for 5 or 12 days reduced peripheral leukocytes and bone marrow cellularity (Farris et al. 1997; Yoon et al. 2001). In the present study, caspase-4 and -12 were significantly activated at the transcription level by benzene exposure particularly in mice lacking the p53 gene. These genes were significantly upregulated in bone marrow by the 12-day benzene treatment. Although these inflammatory caspases were not considerably altered in the benzene-exposed WT mice in this study, our previous study indicated significant upregulation of caspase-4 mRNA when the mice were exposed to 300 ppm of benzene through inhalation (Yoon et al. 2003). This discrepancy might have been due to different protocols for benzene exposure. Thus, both caspase-4 and 12 could be activated by benzene treatment at the transcription level, which is not absolutely dependent upon the p53 gene. Note that lacking the p53 gene exacerbated the activation of the caspase genes in the present study which suggests that the p53 gene might limitedly participate in regulating the expression of the caspases. The alteration of caspase-4 and -12 mRNA did not seem to be associated with cell death since apoptotic evidence was not found in the benzene-exposed bone marrow cells of both WT and p53KO mice. In addition, other apoptosis activator and executioner caspases, such as caspase-9 and -3 were not significantly altered after benzene treatment irrespective of the p53 gene. Although the functional roles and induction mechanisms of caspase-11 and -12 remain

unclear these proinflammatory caspases appear to be activated differentially depending upon the pathogenic situation. In cases of uretic obstruction, these caspases were activated through a p53-dependent pathway (Choi et al. 2001) whereas caspase-12 was activated in a p53-independent manner in the tumor cells infected with an attenuated strain of the Newcastle virus MTH-68/H (Fabián et al. 2007) and in thapsigargin-treated mouse embryo fibroblasts (Li et al. 2006).

The importance of alterations in the caspases at the mRNA level was not determined in the present study because those changes were not further supported by changes in the protein levels of the caspases. The upregulation of mRNA without an increase in proteins might occur without inducing the functional effects on cells such as inflammation and apoptosis. Nevertheless, the changes in caspase-4 and caspase-12 mRNA should be taken into consideration with regard to the action mechanism of benzene. Caspase-4 plays an important role in both inflammation and apoptosis through the activation of caspase-1, which is required for the maturation of proinflammatory cytokines such as interleukin (IL)-1 and -18, which are in turn associated with hyperplasia in myeloid cells (Scott and Saleh 2007). Caspase-4 can also activate caspase-3 which leads to apoptosis under pathological conditions (Fan et al. 2005). In addition, caspase-12, which is highly homologous to caspase-4, is localized in the ER and mediates ER stress-induced apoptosis (Fan et al. 2005). Caspase-12 is also known to be a negative regulator of inflammatory signaling pathways allowing certain cells to survive in the harsh environment created by vigorous inflammatory reactions (Lamkanfi et al. 2007).

In other apoptosis-associated genes, the cell survival genes Bcl2 and Smad6 seemed to be suppressed in response to the 12-day benzene treatment although no significant difference was observed. Bcl-2 suppression at the transcription level was also apparent in previous microarray analyses (Faiola et al. 2004; Yoon et al. 2003), but the implication of suppressing the survival genes is not clear.

Interest is growing as to whether benzene can induce apoptosis in bone marrow cells in association with the benzene-induced hematotoxic and leukemogenic mechanisms. In some previous *in vitro* studies, benzene metabolites induced apoptosis in lymphocytes and HL-60 myeloid leukemia cells (Inayat-Hussain and Ross 2005; Martinez-Velazquez et al. 2006). However, other recent studies have reported contradictory data showing that benzene and/or its metabolites do not induce apoptosis (Faiola et al. 2004; Hazel et al. 1996; Ibuki and Goto 2004). The discrepancy of the previous studies could be associated with the protocol differences; *in vitro* studies usually represent benzene-induced apoptosis while *in vivo* studies including our present study failed to demonstrate evidence of